Sponsored by 🐚

This publication by SEPM Society for Sedimentary Geology
Special Publication No. 99
Application of the Principles Seismic Geomorphology to Continental Slope and Base-of-slope Systems: Case Studies from Seafloor and Near-Seafloor Analogues
and all chapters are available open access (see license terms below) through a financial contribution from Shell.

Open Access Terms

SEISMIC STRATIGRAPHY OF A SHELF-EDGE DELTA AND LINKED SUBMARINE CHANNELS IN THE NORTHEASTERN GULF OF MEXICO

ZOLTÁN SYLVESTER

Shell Research & Development, 3737 Bellaire Blvd., Houston, Texas 77001-0481, U.S.A.
e-mail: zoltan.sylvester@shell.com

MARK E. DEPTUCK

Canada-Nova Scotia Offshore Petroleum Board, Halifax, Nova Scotia B3J 3K9, Canada
e-mail: mdeptuck@cnsopb.ns.ca

BRADFORD E. PRATHER

Shell Upstream Americas, 200 N. Dairy Ashford, Houston, Texas 77079, U.S.A.
e-mail: bradford.prather@shell.com

CARLOS PIRMEZ

Shell Research & Development, 3737 Bellaire Blvd., Houston, Texas 77001-0481, U.S.A.
present address: Shell Nigeria Exploration and Production Company, Lagos, Nigeria
e-mail: carlos.pirmez@shell.com

AND

CIARAN O'BYRNE

Shell Upstream Americas, 200 North Dairy Ashford Road, Houston, Texas 77079, U.S.A.
e-mail: ciaran.obyrne@shell.com

ABSTRACT: The Pleistocene Fuji–Einstein system in the northeastern Gulf of Mexico consists of a shelf-edge delta that is directly linked to and coeval with two submarine channel–levee systems, Fuji and Einstein. There is a continuous transition between the channel fills and the delta clinoforms, and the seismic reflections of the prodelta are continuous with the levee deposits. Five smaller delta lobes within the Fuji–Einstein delta formed through autocyclic lobe switching that was superimposed on a single falling-to-rising sea-level cycle. The corresponding stratigraphic complexity is difficult to interpret in single downdip seismic sections, especially where elongated mudbelts are attached to some of the delta lobes. The two slope channel systems, Fuji and Einstein, deeply incise the shelf-edge delta. However, late-stage delta progradation was coeval with slope-channel development, and, as a result, there is no easily mappable, single erosional surface separating channel deposits from deltaic sediments. During early delta-lobe development, a gully field forms on the upper slope, directly downdip from the delta lobe. As the delta progrades, one of the larger gullies in the middle of the field captures most of the denser flows and gradually evolves into a sinuous channel. The larger delta-related slope channels source 2–4 km-wide submarine aprons where they encounter areas with lower gradients. If the slope gully or channel remains active for a long enough time, its corresponding submarine apron smooths out the slope and becomes incised by the later bypassing flows. The well-preserved and mappable 3D shelf-edge architecture provides a rare opportunity to understand relationships between deltaic and slope depositional systems.

Key words: shelf-edge delta, submarine channel, turbidity current, sequence stratigraphy, slope deposits, channel–levee system, mudbelt, slope apron

INTRODUCTION

Shelf-edge deltas (SEDs) are sites of thick sediment accumulation near the continental shelf edge, deposited during times of shelf exposure due to either (1) lowering of eustatic sea level (i.e., a forced regression), or (2) filling of shelf accommodation in times of stable sea level, slow subsidence, and high sediment supply (i.e., a highstand systems tract that reaches the continental shelf edge; Posamentier et al., 1992; Burgess and Hovius, 1998). SEDs may contain good-quality reservoirs and represent an important hydrocarbon play around the world (e.g., Meckel, 2003; Sydow et al., 2003; Cummings et al., 2003). In addition, they locally serve as the main sediment input point for associated deep-water depositional systems, including canyons, channels, slope aprons, and basin-floor fans, often significant exploration targets themselves (Pettingill and Weimer, 2002). Development of SEDs is strongly influenced by sea-level history, and hence correlating SEDs to fan systems should provide a better understanding of sea-level controls on fan deposition. Such correlations should also lead to improved prediction of reservoir presence and architecture.

With improvements in seismic technology and increased availability of high-quality 2D and 3D seismic datasets, our understanding of deltaic and submarine slope depositional systems has increased considerably in recent years (e.g., Pirmez et al., 2000; Deptuck et al., 2003; Deptuck et al., 2007; Saller et al., 2004; Adeogba et al., 2005; Rabineau et al., 2005; Pirmez et al., this volume; Prather et al., this volume). However, most studies focus either on the delta or on the turbidite system and stop short of investigating in detail the linkage between the two. With a few exceptions (e.g., Saller et al., 2004), papers that specifically address links between deltas and submarine fans commonly lack three-dimensional data coverage, which hinders both seismic-based (e.g., Berryhill et al., 1986; Roberts et al., 2004; Suter and Berryhill, 1985, Gervais et al., 2004, Deptuck et al., 2008) and

outcrop-based (e.g., Mellere et al., 2002; Plink-Björklund and Steel, 2005) studies. In fact, we are not aware of any examples where a delta has been analyzed in full detail in three dimensions. The prevalence of growth faults and sediment failures, in addition to the complex patterns of delta-lobe avulsions, further obscures correlation between deltas and fan systems and increases the need for three-dimensional coverage.

In this study, we explore the relationship between SEDs and submarine channels in the northeastern Gulf of Mexico, in an area of limited deformation and shallow burial. Widespread high-quality 3D seismic coverage, combined with high-resolution 2D seismic profiles and limited coring, allows detailed study of the Fuji–Einstein shelf-edge delta and two related slope channel–levee systems. The main goal of this study is to describe the seismic stratigraphy and morphology of both this shelf-edge delta and a directly linked turbidite system deposited on a nearly graded slope (*sensu* Prather, 2003). The slope channels and aprons in the study area are analogues for reservoirs in similar settings, for example the Ram Powell and Tahoe fields, containing Miocene reservoirs in the Eastern Gulf of Mexico (e.g., Clemenceau, 1995; Kendrick, 2000). Using basic stratigraphic concepts and detailed seismic interpretation, we attempt to unravel the sea-level history and use this information to improve our understanding of outer-shelf and upper-slope processes involved in construction of shelf-edge deltas and initiation of submarine channels.

The terms "channel", "channel–levee system," and "slope apron" are used throughout this paper. Single-thread submarine channels are distinct from "channel belts" or "submarine valleys" (Prather, 2003), which are larger and consist of more than one spatially and genetically associated channel form. The channelized components of the Fuji and Einstein systems discussed in this paper clearly consist of multiple channel threads and therefore would qualify in such classification schemes as "channel belts" or "valleys". However, the systems described here represent an early stage of evolution from a single thread to multiple threads, and show evidence of a full continuum between single slope gullies with low sinuosity and migrating channels with significant sinuosity. Because we want to emphasize this continuum, and for sake of simplicity, in this paper we use the terms "channel" and "channel–levee system" when referring to the channelized parts of the Fuji and Einstein systems that formed on the slope.

We use the term "slope apron" to describe deposits forming on the slope in locations where the gradient is reduced and slope channels or gullies pass into unconfined, laterally more extensive, usually relatively sand-rich and therefore higher-amplitude deposits. For a detailed discussion of related terms, see Prather et al. (this volume).

GEOLOGIC SETTING

The Mississippi–Alabama shelf break in the northeastern Gulf of Mexico (Fig. 1) has prograded more than 50 km to the south and southeast since the Miocene (Godo, 2006). Between the Mississippi Delta and the head of the De Soto Canyon, a number of bathymetric lobes of variable size characterize the outer shelf and uppermost slope (Fig. 2; Gardner et al., 2007). They represent the draped sea-floor expression of SEDs that were probably deposited during periods of falling Pleistocene sea level (McBride et al., 2004). Seaward of the SEDs, several morphologic features are recognized on the sea floor, including slope gullies, channels and canyons, slide scars and associated mass-transport deposits, and salt diapirs (Fig. 2). Dorsey Canyon and Sounder Canyon are the most prominent slope valleys , but other erosional features are

also recognized on the slope, including the study area, where increased burial depths have decreased their relief (Fig. 2).

This study focuses on the Fuji–Einstein delta, located on the outer shelf to upper slope in the northeastern Gulf of Mexico, about 230 km southeast of New Orleans and 180 km south of Mobile, Alabama (Fig. 1), and the time-equivalent strata in deeper water outboard of it. Two slope channels (Fuji to the west and Einstein to the east) are recognized in front of the delta and were mapped over straight-line distances of about 75 km from the paleo–shelf edge to water depths of 2300 m. On the continental rise, both systems are buried by younger deposits or were obliterated by large slope failures (Fig. 2). Several slide scars are present on the upper slope. The youngest, located east of the Einstein channel, is most prominent (Fig. 2). It is associated with a large mass-transport complex (MTC) on the lower slope, recognized by its irregular surface morphology.

Three salt diapirs (3 to 5 km in diameter) form prominent positive bathymetric elements on the sea floor to the west of the Fuji and Einstein channels, and a fourth, smaller, one is present near the upper part of the Fuji channel. A number of normal faults are also present near the shelf edge. Fault scarps are not visible on the sea floor, but the faults are apparent in dip seismic sections (Fig. 3). Their deepest parts typically reach a prominent seismic reflection (marked as 'Top Chalk' in Figure 3) that corresponds to the boundary between the siliciclastic Miocene and the marl- and chalk-dominated Lower Tertiary rocks (Godo, 2006). Large faults beyond the present-day shelf edge tend to be counter-regional, in contrast with most faults on the shelf, which are dipping toward the basin.

PREVIOUS WORK AND PRESENT DATASET

The Fuji–Einstein system has been the subject of a number of studies since the late 1980s. Initial mapping of the system was done by Shell geoscientists (Winker, 1993a, 1993b; Hackbarth and Shew, 1993; Hackbarth and Shew, 1994), who used the Einstein Channel as an analogue for more deeply buried submarine channel reservoirs. Later studies largely focused on aspects of channel evolution (Faulkenberry, 2004), combined with sequence stratigraphic interpretations (Posamentier, 2003; Catuneanu, 2006).

Of particular importance to this study is the work of Winker (1993a, 1993b), who mapped both the Fuji and Einstein channel–levee systems and the associated delta lobes and highlighted the sequence stratigraphic relationships between them. Winker (1993a) observed that each shelf-margin delta (or delta lobe) and its corresponding slope channel form a regionally mappable seismostratigraphic unit. In contrast, the erosional surfaces that mark the channel-head incision separating the underlying deltas from the channel-head incisions are not regionally mappable.

Hackbarth and Shew (1993, 1994) used a regional grid (spaced 5–8 km) and a tighter grid (spaced 60–300 m) of high-resolution 2D seismic profiles to study the Einstein channel. In addition, three shallow boreholes were drilled into the channel and its levees, were logged, and in some intervals cored. A number of seismic facies were distinguished and were calibrated with well data.

Posamentier (2003) relied on more recent 3D seismic data, and emphasized that the slope channels (called Channel "E" and Channel "W", respectively, for the Einstein and Fuji channels of Hackbarth and Shew, 2004) were probably created by hyperpycnal flows, suggested that the evolution of the delta and channel-levees was strongly linked to a single lowstand cycle, and determined that delta progradation was coeval with the development of sinuous channels on the slope.

The present study builds on these results, mainly through additional seismic mapping of high-quality 3D seismic data. Our
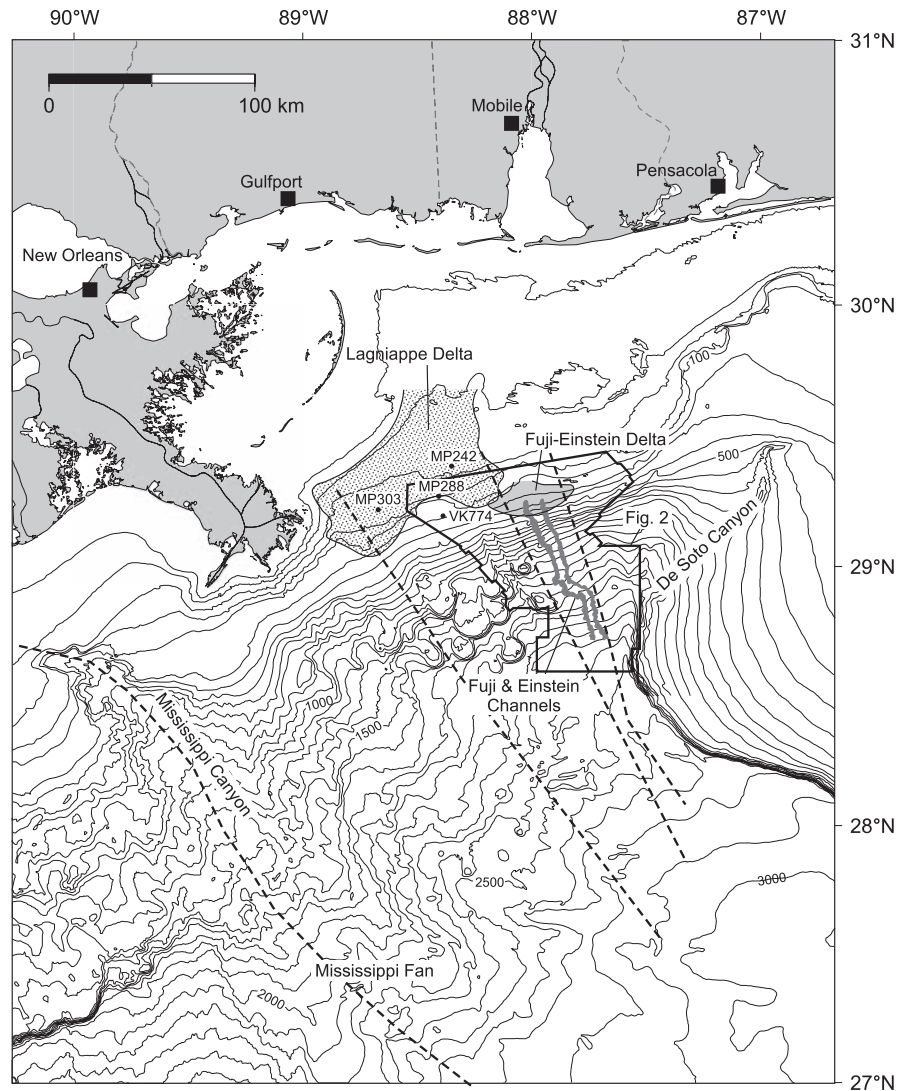
FIG. 1.—Seafloor morphology and location of the Fuji–Einstein system in the northeastern Gulf of Mexico. Outline of Lagniappe delta is from Roberts et al. (2004). Dashed lines show locations of topographic profiles in Figure 29A.

primary dataset consists of three contiguous 3D seismic volumes of variable quality. The data volume covering the delta and the upper slope has a significantly higher signal-to-noise ratio than the other two volumes, and most of the key observations refer to this high-quality dataset (Fig. 2). The highest frequency content of this seismic volume in the near-seafloor zone is about 60 Hz; a typical interval velocity of 1700 m/s yields a resolvable limit of about 7 m. The seismic bin spacing is 25 m x 25 m. Apart from a prominent seafloor multiple, data quality is remarkably good. We also use the three research wells drilled in the Einstein channel-levee system and an additional industry well to calibrate the seismic dataset (see also Hackbarth and Shew, 1994).

SEISMIC MORPHOLOGY AND STRATIGRAPHY OF THE FUJI–EINSTEIN DELTA AND RELATED DEPOSITS

The Fuji–Einstein delta is one of the most distal SEDs on the present-day upper slope in the northeastern Gulf of Mexico (Fig. 2). The base and top surfaces of the Fuji–Einstein delta are well defined in the 3D seismic volume and were mapped across most of the study area (Figs. 4, 5). Seismostratigraphic surfaces internal to the system have smaller areal extents but were also correlated with confidence. The delta extends about 40 km along strike and 20 km in the dip direction (Fig. 6). Its maximum time thickness is 360 ms (TWTT) or about 313 m (using an interval velocity of 1740 m/s).

Age Constraints

Precise dating for the Fuji–Einstein delta is not possible with the available data, but indirect lines of evidence help constrain its age. We have used its stratigraphic position relative to other deltas, combined with extrapolations of sedimentation and subsidence rates from better constrained systems, to estimate its age. The delta is not visible on the present-day sea floor because it is buried by up to 300 m of sediment at the paleo–shelf edge. However, its stratigraphic position indicates that it is older than the deltas of the eastern Gulf of Mexico described in Anderson and Fillon (2004). It is also older than the Dorsey–Sounder delta (Fig. 2). Roberts et al. (2004, their Figure 33) suggest that this delta
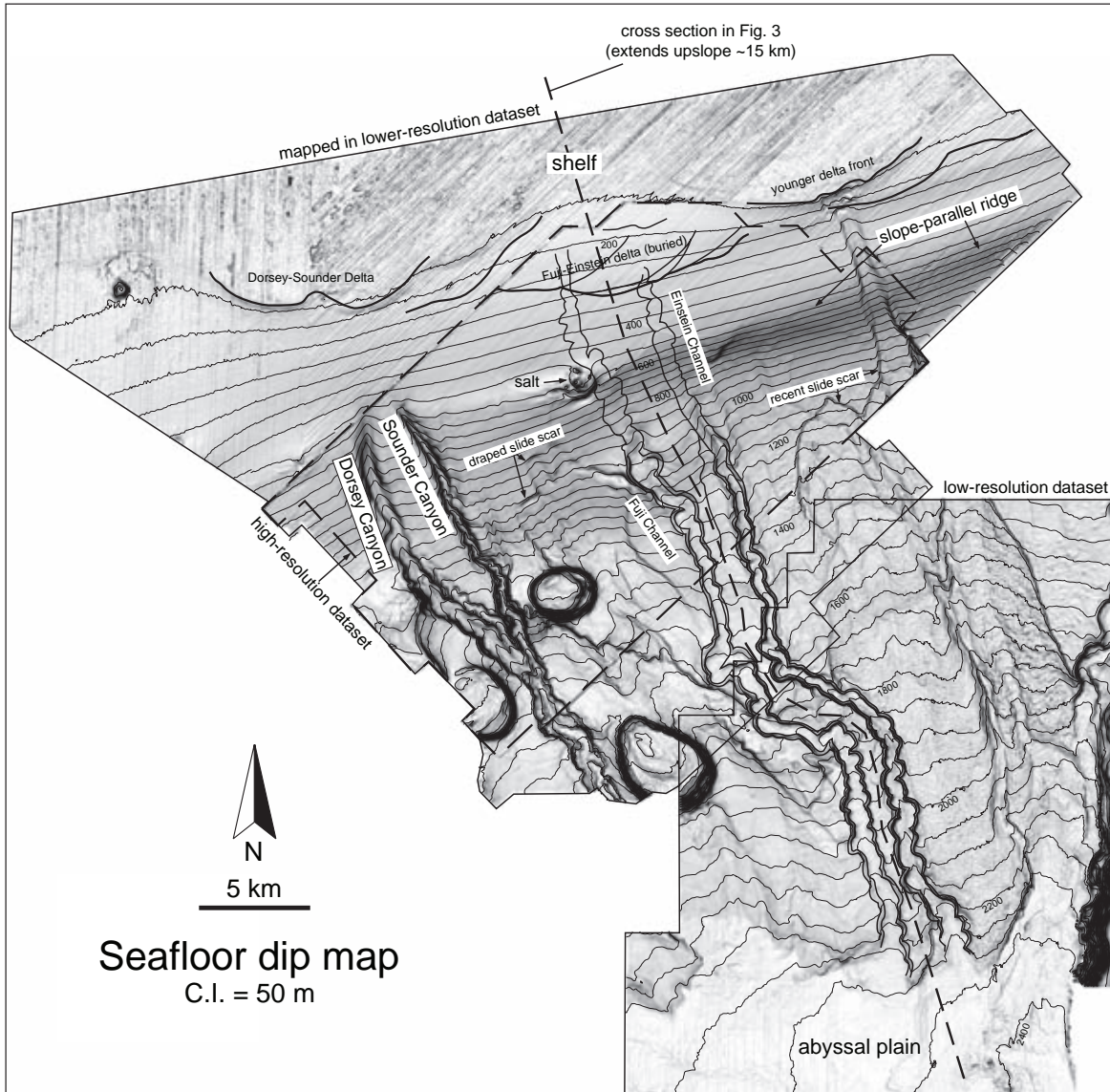
FIG. 2.—Seafloor dip-magnitude map of the area around the Fuji–Einstein delta and channels, with outlines of the seismic data volumes used in this study.

was deposited during Marine Isotope Stage (MIS) 8. The stratigraphic architecture, distal location, and comparison with other SEDs of known age in the area suggest that the Fuji–Einstein delta formed during one sea-level lowstand; this lowstand must be older than MIS 8.

Additional age constraints come from estimating the subsidence rate in the area and comparing it with the present-day depth of the Fuji–Einstein shelf break. The offlap break of a shelf-edge delta penetrated by the research corehole VK774c1 (Fig. 1), at a total depth of 232 m below present-day sea level, has an age of ~ 250 ky (end of MIS 8; Fillon et al., 2004). Assuming that the offlap break formed close to the paleo-shoreline and a paleo–sea level of -80 m, the average subsidence rate at this location was about 0.6 mm/year. This is consistent with long-term subsidence rates of about 0.5 mm/year in the eastern Gulf Of Mexico (Anderson and Fillon, 2004, their Table 1). Taking into account the present-day depth of the Fuji–Einstein offlap

break (~ 400 m below sea level, with some variability across delta lobes), a likely range of paleo-sea-level values (-60 m to -120 m, assuming deposition during a glacial lowstand), and a reasonable range of subsidence rates (0.4 to 0.7 mm/yr), the Fuji–Einstein delta is likely older than 400 ky but younger than 850 ky (Fig. 7). This interval includes the glacial lowstands corresponding to MIS 12 to MIS 20. Subsidence rates larger than 0.7 mm/yr could bring the age of the delta down to MIS 10 (Fig. 4), but the age constraint given by the Dorsey–Sounder delta (of age MIS8) would still apply.

Delta Lobes and Clinoforms

Description.—

On dip sections, the internal architecture of the Fuji–Einstein delta is dominated by prograding clinoforms that reflect the
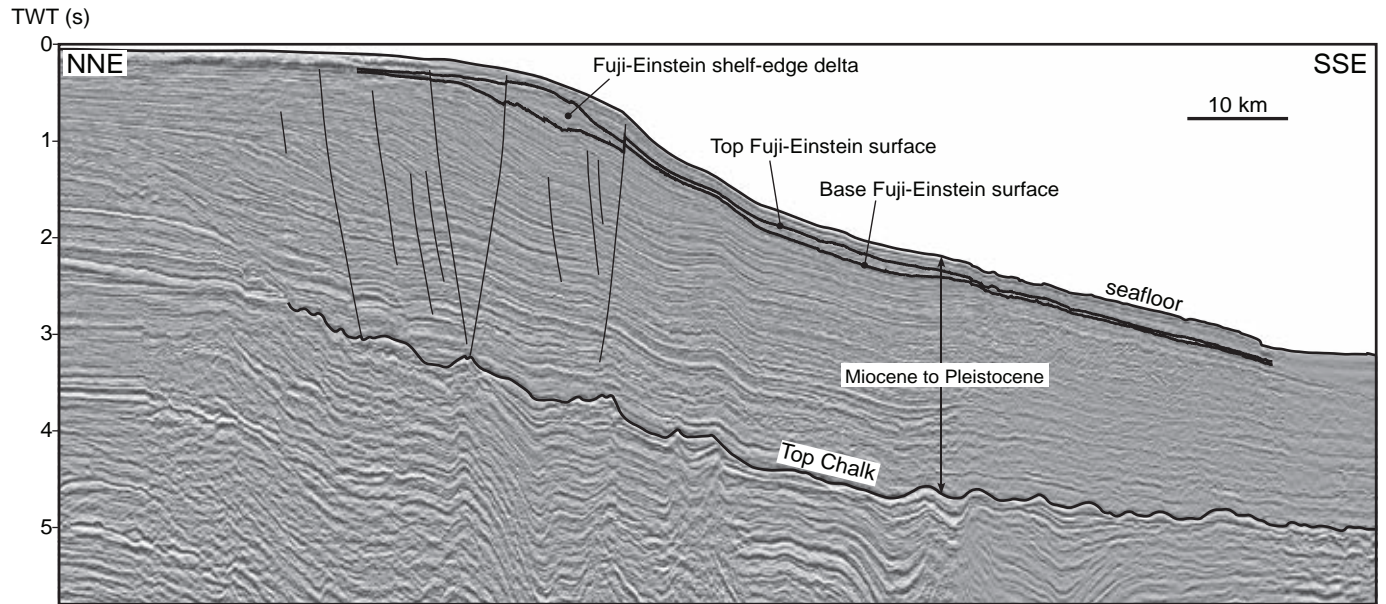
FIG. 3.—Large-scale cross section between Fuji and Einstein Channels (see Figure 2 for location). Seismic data courtesy of CGG Veritas.
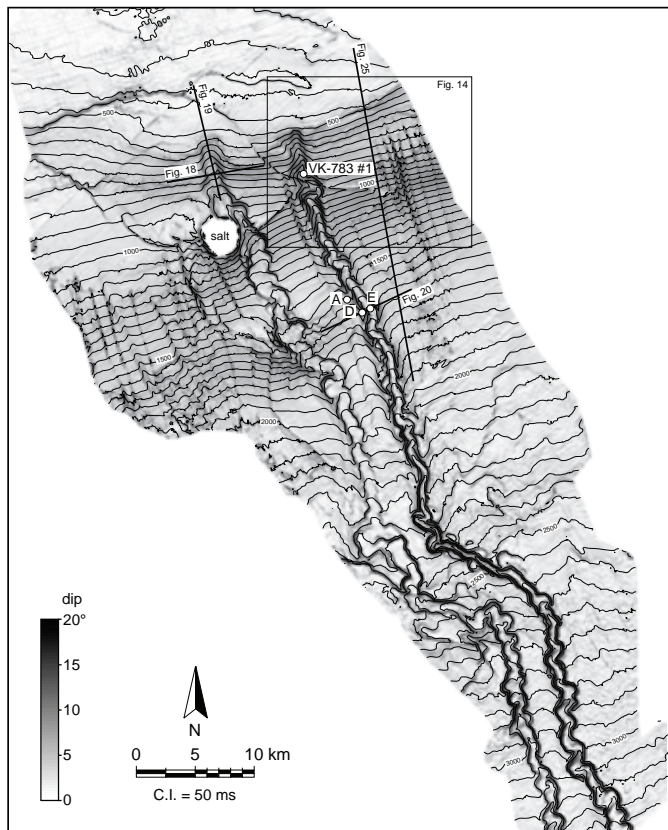

FIG. 4.—Time structure (contours) and dip magnitude (gray shades) map of top Fuji–Einstein surface. A, D, and E mark the locations of Shell research wells.
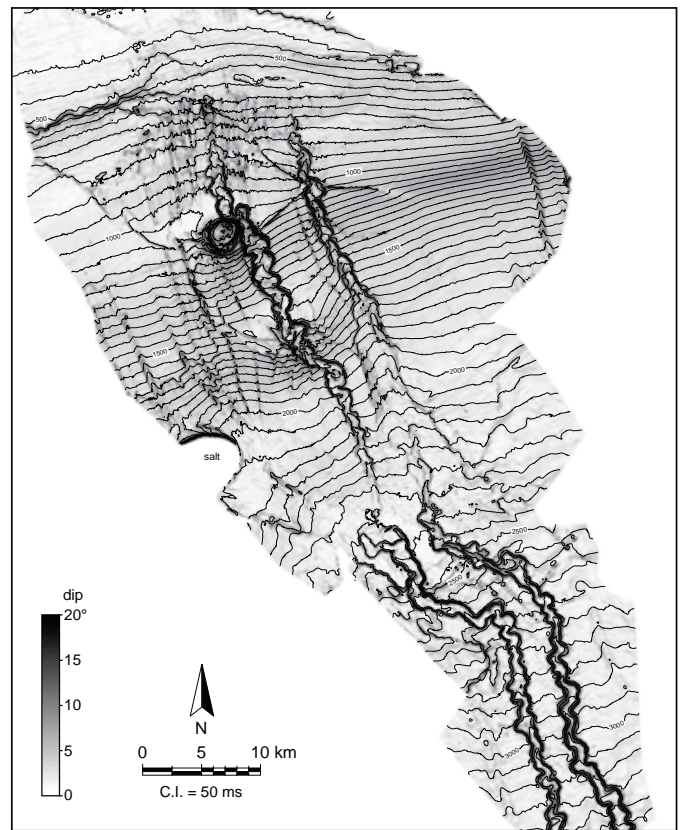
FIG. 5.—Time structure (contours) and dip magnitude (gray shades) map of base Fuji–Einstein surface. Incision of the slope channels is pronounced on the upper slope; it decreases in the central part of the mapped area, then it increases again downdip from there.
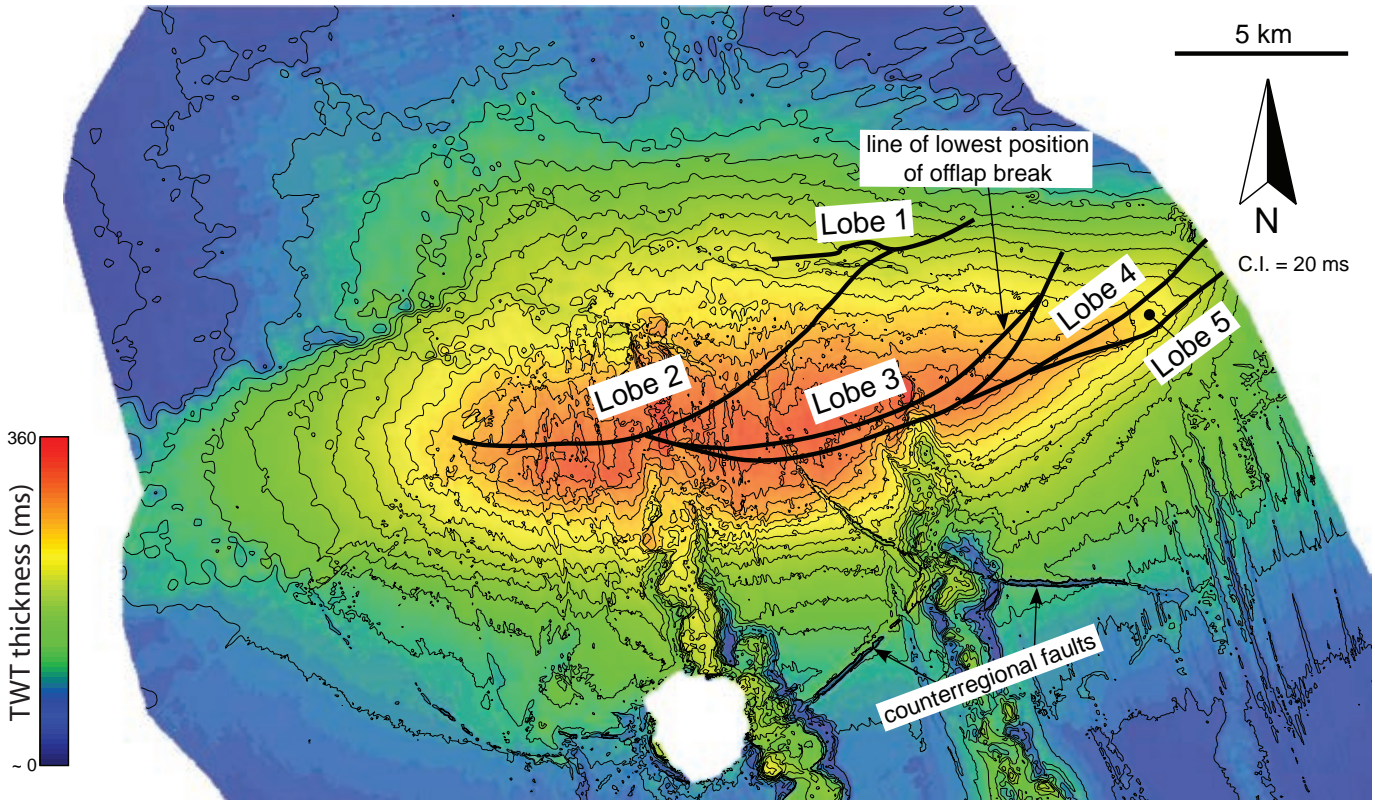
FIG. 6.—Thickness map of the Fuji–Einstein delta. Thick black lines mark the most basinward offlap breaks of the delta lobes.
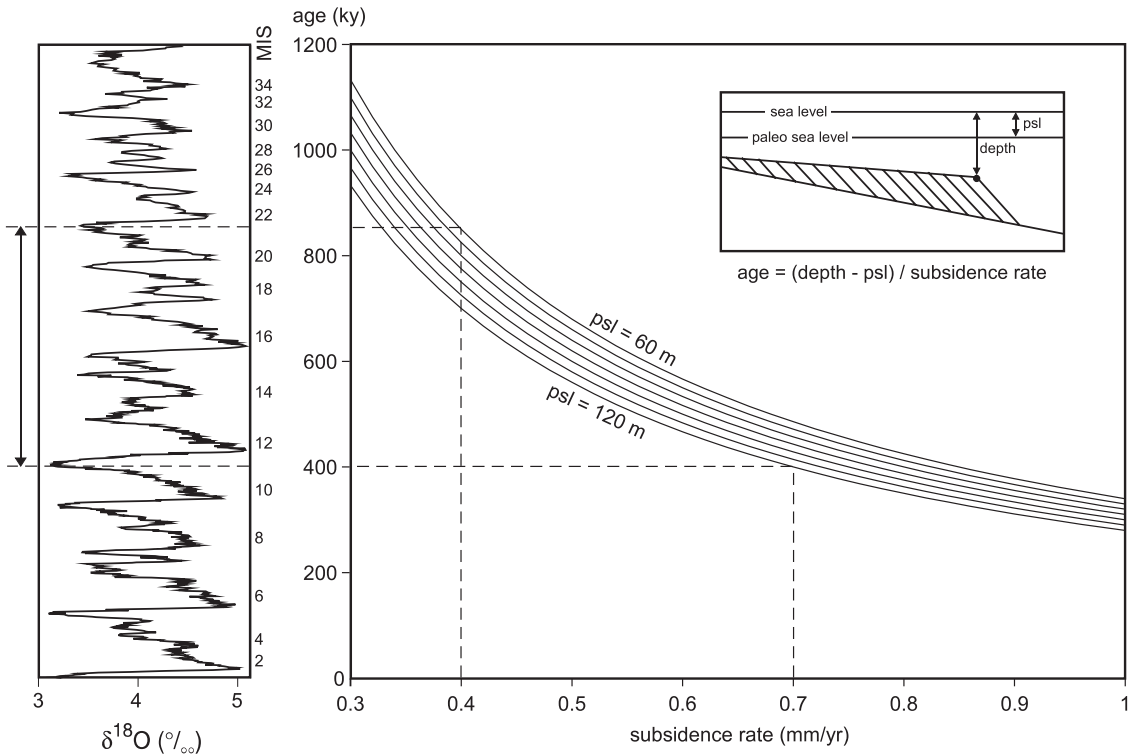

FIG. 7.—Age constraints for the Fuji–Einstein delta: age as a function of subsidence rate and paleo–sea level. Oxygen isotope curve is from Lisiecki and Raymo (2005).

overall seaward advance of the offlap break, with late-stage aggradation of the delta top. On strike sections, the delta has a broad lens-shaped external form. Internal seismic reflections are truncated by erosional surfaces, and detailed inspection reveals several onlap and downlap surfaces. Three-dimensional mapping of these surfaces indicates the presence of a number of smaller-scale delta lobes, and hence progradation of the Fuji–Einstein delta is overprinted by the effects of delta-lobe switching and the presence of erosional canyon heads that extend back onto the delta platform.

Five delta lobes were identified and mapped in the Fuji–Einstein delta (Fig. 6). These lobes are numbered in chronological order and are color-coded in maps and cross sections. Lobes 2 and 3 are the largest ones, and they link downdip to the Fuji and Einstein channels, respectively (Figs. 8, 9). Interpretations are based on three-dimensional mapping of the bounding surfaces. A number of interpreted cross sections and time slices are shown in Figures 8, 10, 11, and 12. The three dip sections in Figure 8 were chosen so that they avoid the stratigraphic complexity of the Fuji and Einstein canyon heads.
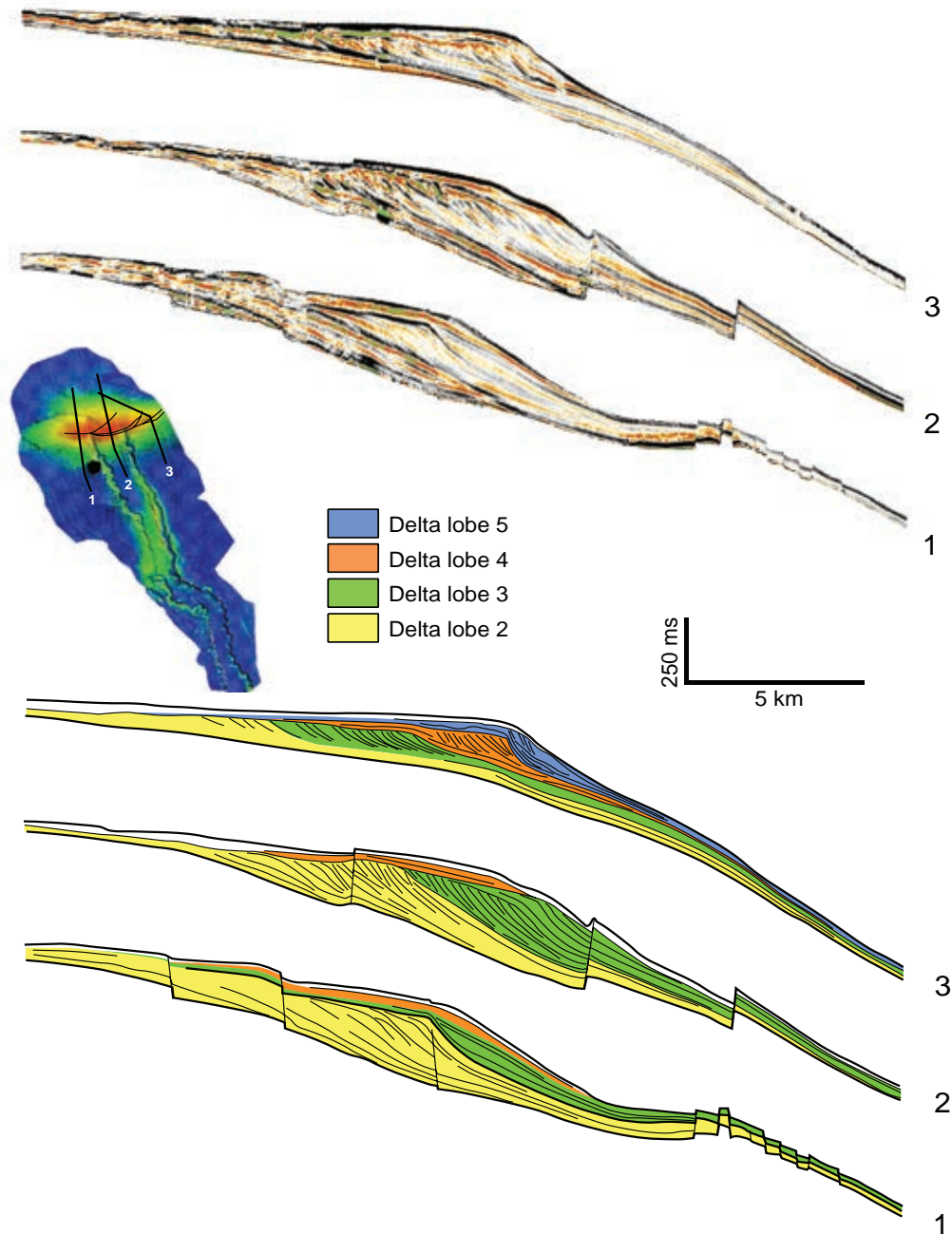

FIG. 8.—Seismic and interpreted dip sections across the Fuji–Einstein delta (only seismic data between base and top Fuji–Einstein surfaces is shown). Seismic data courtesy of CGG Veritas.
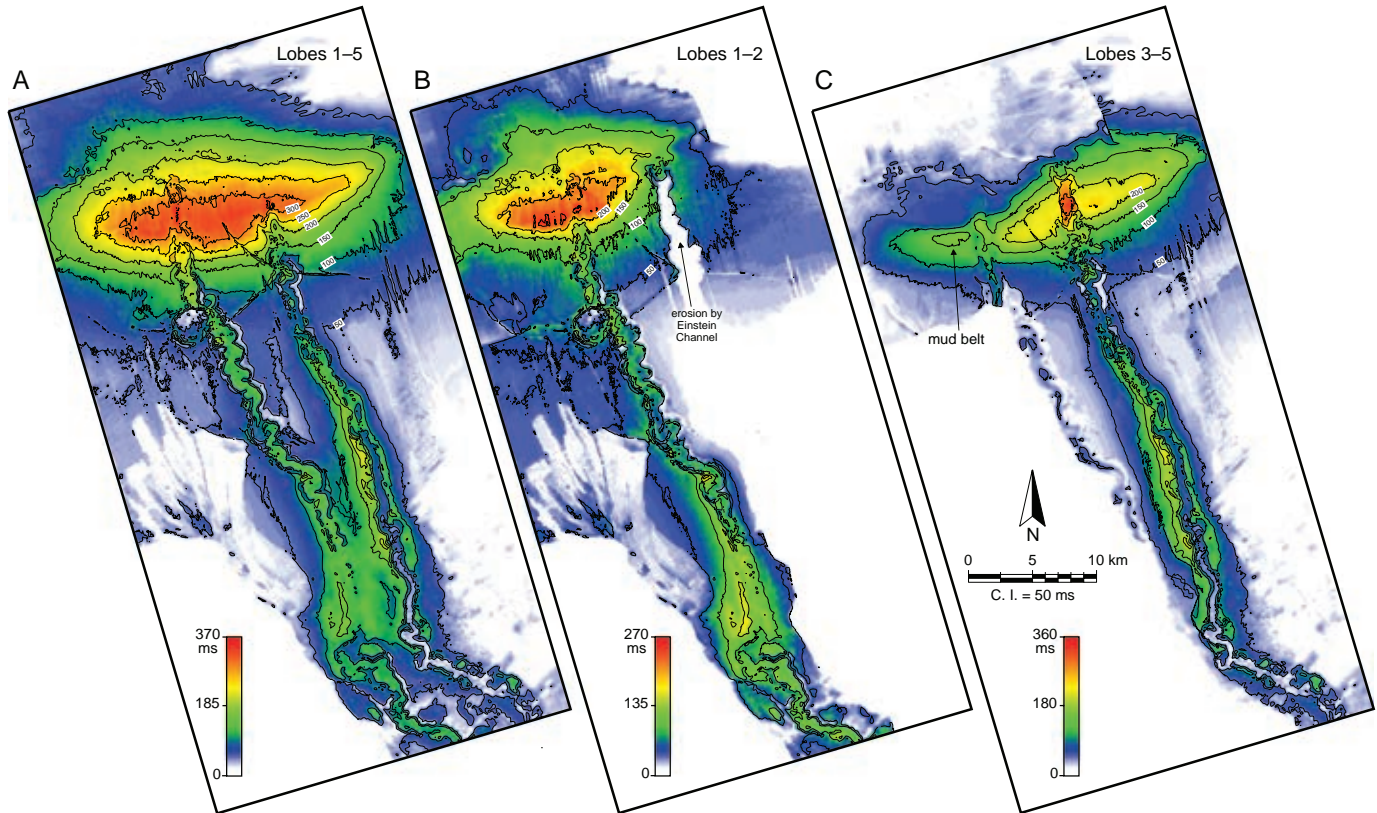
FIG. 9.—Thickness maps showing that the slope channels are partially coeval with the delta lobes. **A)** Thickness map of the stratigraphic interval that corresponds to the Fuji–Einstein Delta (lobes 1–5) and to Fuji and Einstein Channels. **B)** Thickness map of lobes 1 and 2 and Fuji Channel. This interval is dominated by lobe 2. **C)** Thickness map of lobes 3 to 5 (dominated by lobe 3) and Einstein Channel.

Lobe 1 was deposited first and could be mapped only in the highest-resolution seismic volume (Fig. 2). A strong sea-floor multiple obscures a large part of this lobe, but it has well preserved topsets and was mapped along strike for 7 km, with clinoforms extending up to 2 km in the dip direction. Seismic attribute maps, especially trace-shape maps, show N–S-oriented, slightly curved linear features on the top surface of delta lobe 1 (Fig. 13). The majority of these channel-like features in the center of the image converge toward an ~ 1-km-wide slope-channel head that narrows in a downslope direction into a 100-m-wide channel. Some of the delta-top channels pass seaward into the slope channel without any visible discontinuities. Another bundle of delta-top channels is present to the east. These channels converge toward a younger slope gully that is not visible on the mapped clinoform (Fig. 13).

Lobe 2 was deposited to the west and seaward of lobe 1 and extends for more than 23 km along strike and 14 km in the dip direction, and is the largest in terms of both its volume and its areal coverage (Figs. 6, 8, 11, 12). At its apex, this lobe links to the Fuji Channel through a submarine canyon head. Although an erosional surface is present at the base of the canyon, this surface terminates against the delta top and no obvious fluvial incision can be mapped at the delta top. Landward of the offlap break, lobe 2 has an irregular top surface dominated by downstepping clinoforms. Seismic attribute maps of these surfaces show no obvious patterns indicative of fluvial channels. The upper parts of the clinoforms show amplitude patterns that are more consistent with beach ridges formed along a wave-dominated coast (Fig. 12).

Lobe 3 was deposited east of lobe 2, is only slightly smaller than lobe 2, and links to Einstein Channel on the slope. In time slices, the topmost parts of the lobe 3 clinoforms show up as SW–NE-oriented, high-amplitude reflections. These reflections become lobate in shape and of lower amplitude in their deeper parts (Fig. 12). In dip sections, most clinoforms are oblique but become more sigmoidal through time. Similarly to lobe 2, the top surface of lobe 3 is irregular and is dominated by the downstepping clinoforms. The high-amplitude uppermost parts probably represent sandy beach ridges.

Lobes 4 and 5 are both smaller (~ 6 km width) than lobes 1 and 2, and are situated east of lobe 3. No large submarine channels link to these smaller lobes; instead, a well-developed gully field that links to Lobe 5 is apparent on the top Fuji–Einstein surface (Figs. 4, 6). During deposition of lobes 4 and 5, small deltas partially filled the submarine channel heads that incise into lobes 2 and 3 (Figs. 11, 12).

Interpretation.—

One cannot rule out the possibility that increased sediment supply caused progradation of the Fuji–Einstein delta onto the upper slope, but it is unlikely that rivers could focus sediment to relatively small depocenters on the outermost shelf during periods of high eustatic sea level. Overall, the three dip sections in Figure 8 suggest that the Fuji–Einstein delta was deposited during a single falling-to-rising eustatic sea-level cycle. In section 2 of Figure 8, consecutive reflections that belong to lobes 2
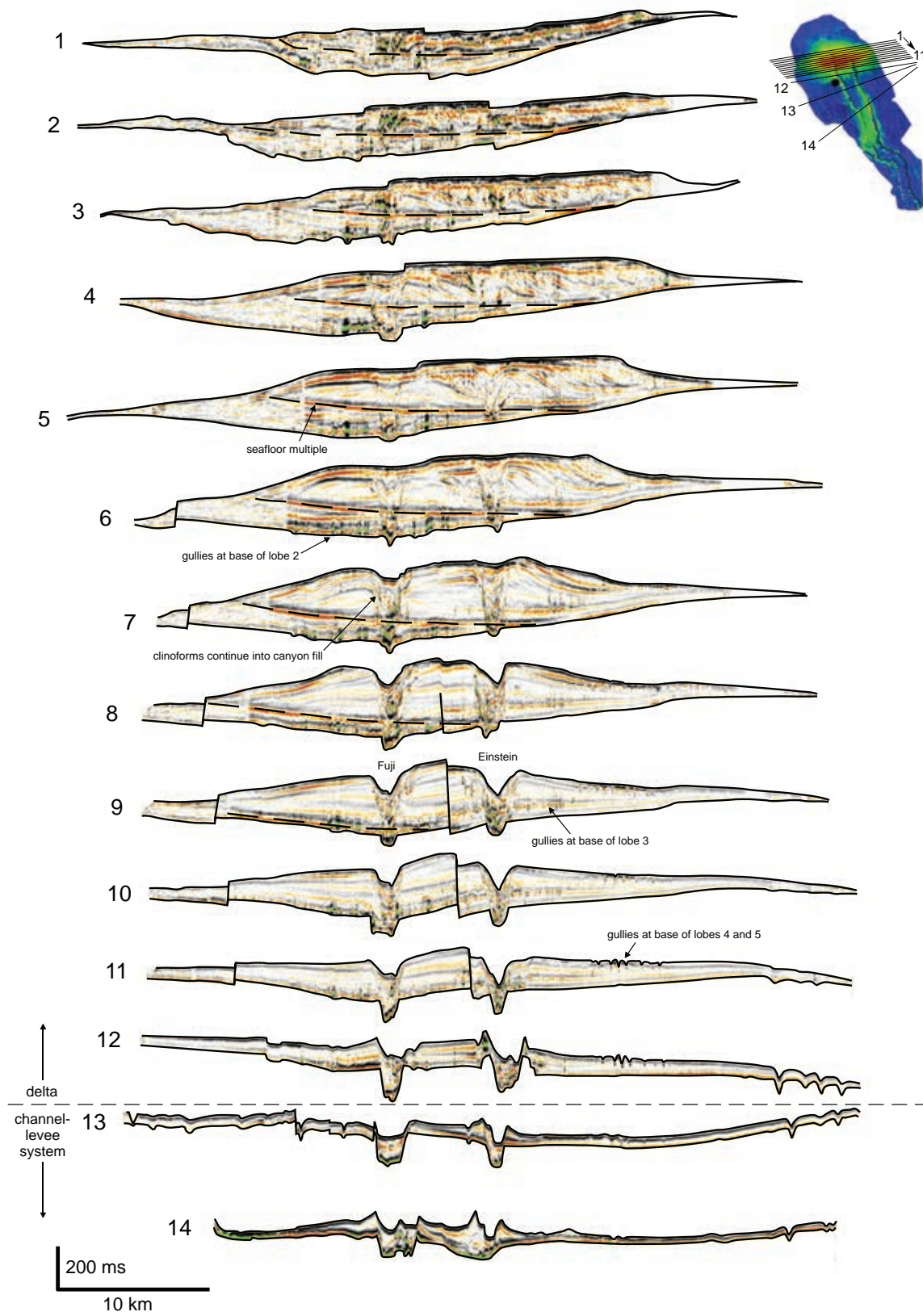
Fig. 10.—Seismic strike sections across the Fuji–Einstein delta and channel–levee systems (only seismic data between base and top Fuji–Einstein surfaces is shown). Seismic data courtesy of CGG Veritas.

Delta lobe 5
Delta lobe 4
Delta lobe 3
Delta lobe 2

200 ms

10 km

FIG. 11.—Interpreted strike sections across the Fuji–Einstein system.

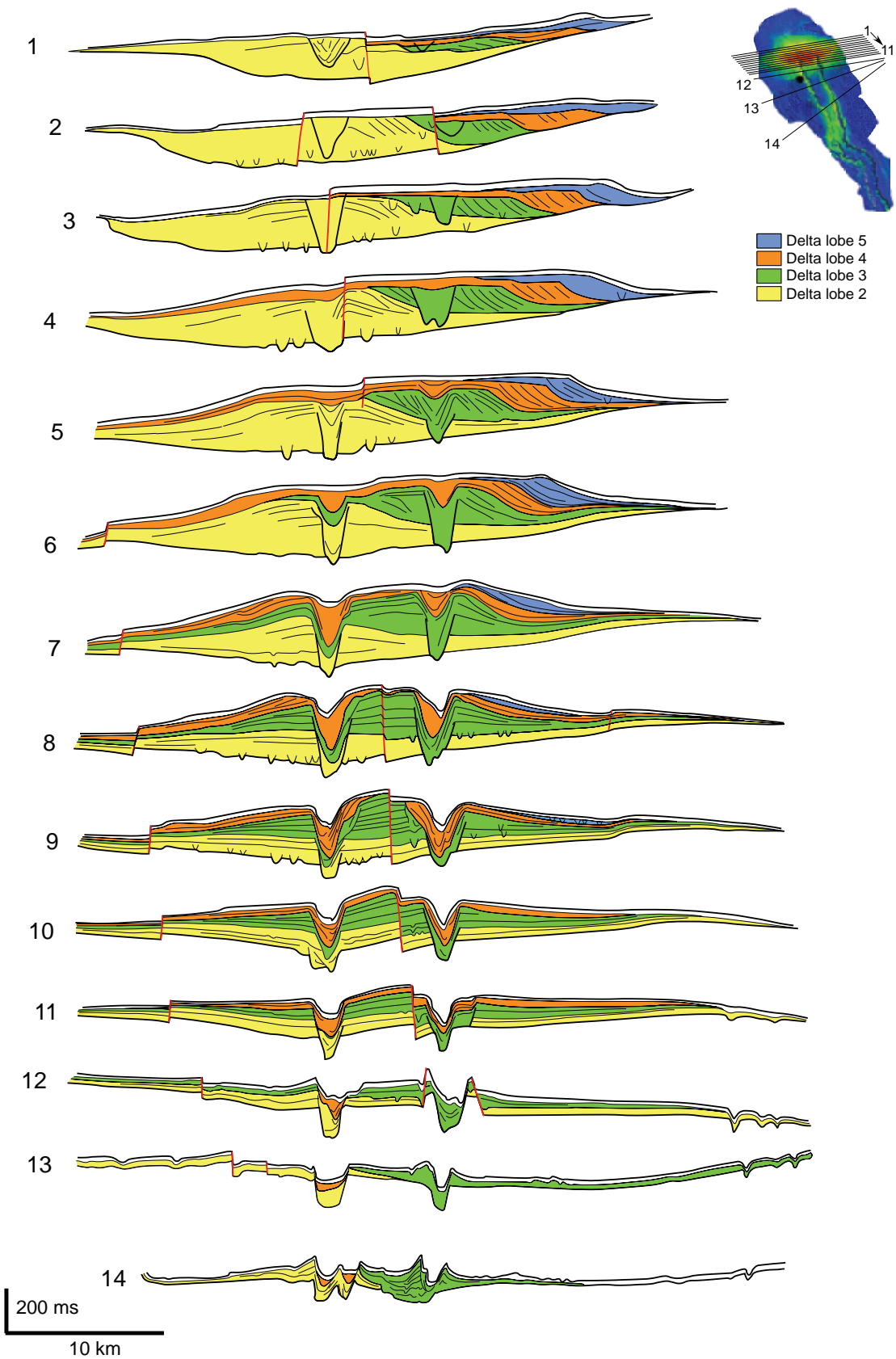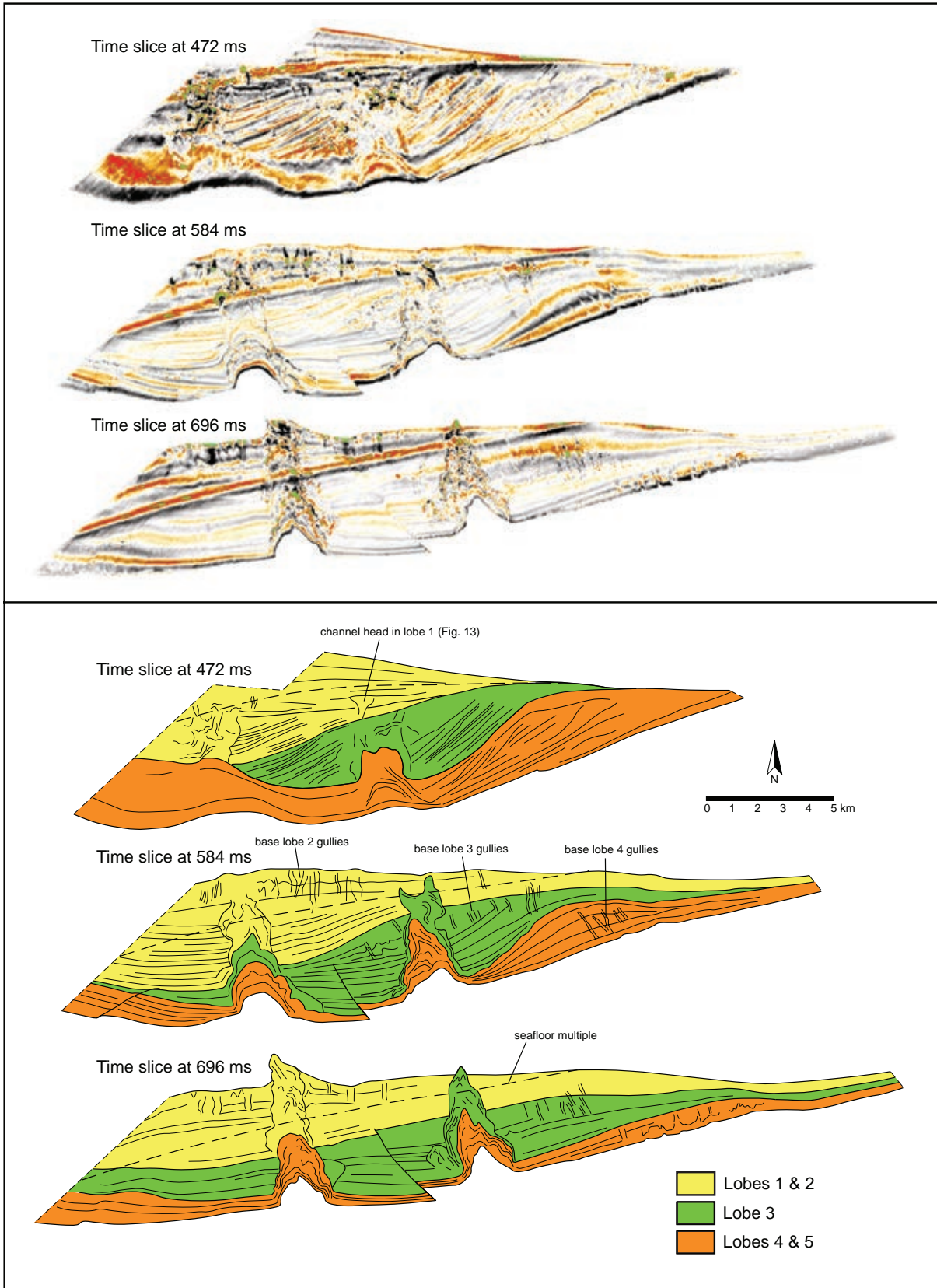FIG. 12.—Uninterpreted and interpreted time slices of the Fuji–Einstein delta (only seismic data between base and top Fuji–Einstein surfaces is shown). Seismic data courtesy of CGG Veritas.
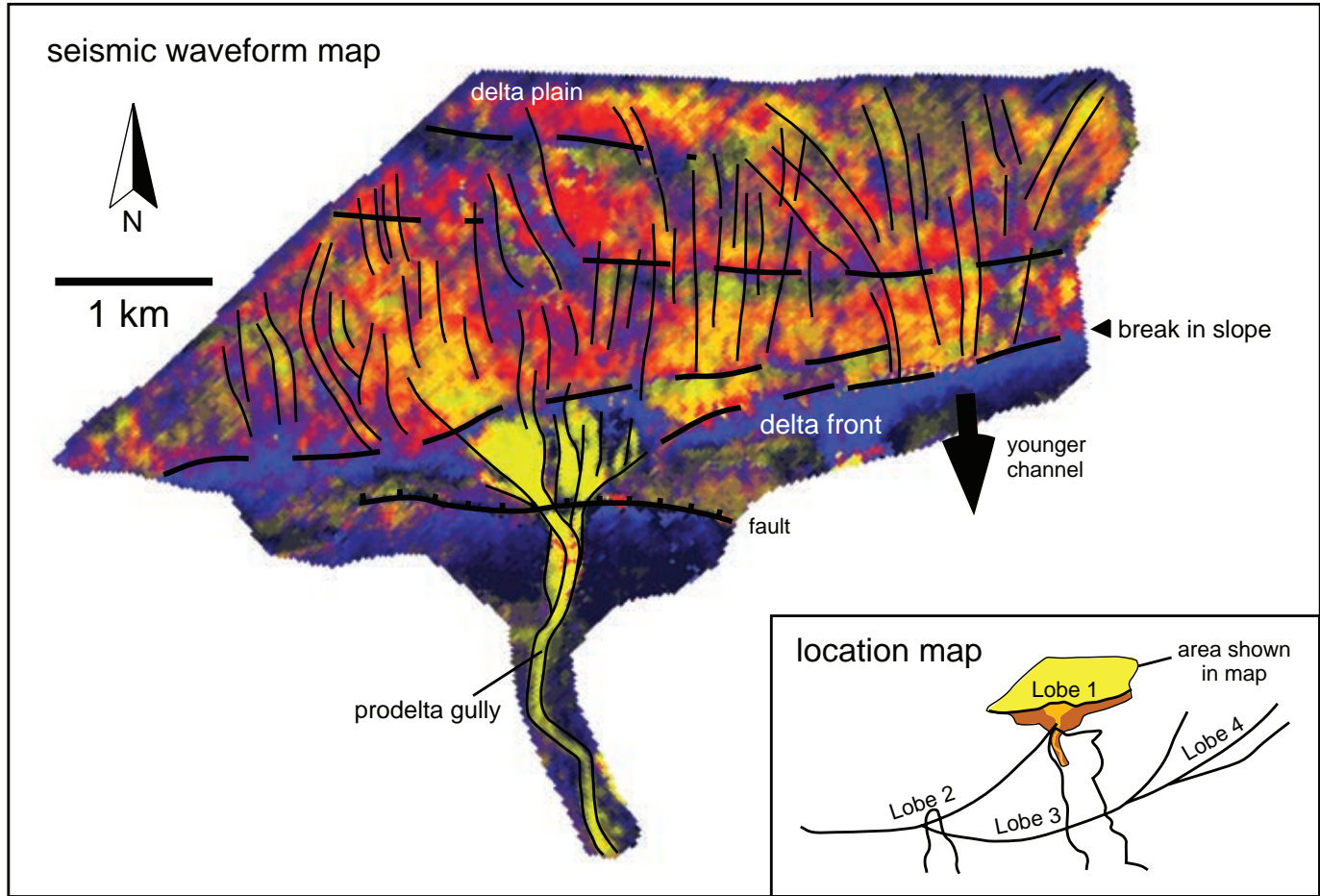
Fig. 13.—Seismic trace-shape map of top of the oldest delta lobe. Linear features are probably fluvial distributary channels that seem to be converging toward and directly linked to slope gullies.

and 3 terminate against the previous ones at slightly lower levels, with local erosional truncation. This geometry suggests that both lobes 2 and 3 were deposited during a forced regression (Posamentier et al., 1992). The offlap break and the shoreline trajectory indicate that sea level rose again toward the end of deposition of lobe 3, and lobes 4 and 5 were deposited during an overall rising relative sea level. It is possible that minor forced regressions were superimposed on the rising trend (especially during lobe 4 time; section 3 in Figure 8). The heads of the submarine channels cutting into lobes 2 and 3 appear to have been reactivated and partially filled with canyon-head deltas during deposition of lobes 4 and 5. The internal architecture of the delta reflects an overall regressive-to-transgressive evolution, strongly overprinted with the effects of autocyclic lobe switching. There is no evidence that lobe switching was triggered by sea-level changes.

A comparison of section 1 with section 2 shows that relative-sea-level change can be variable even within a relatively small delta. In section 1, relative sea level began to rise immediately after deposition of lobe 2 ceased, that is, slightly sooner than it does in section 2, and a thin deposit on top of lobe 2 in this western area correlates to lobe 3 to the east. This difference is probably due to more pronounced subsidence in the area of the thick Lobe 2, especially to the southwest of the large growth fault that was active during deposition of Lobe 2.

Slope Gullies

Description.—

A large number of predominantly erosional slope gullies are present at several stratigraphic levels in the study area. They are typically clustered into fields covering relatively small areas of the slope at specific stratigraphic levels. These gully fields consist of several straight, parallel, and largely erosional features oriented orthogonal to the slope. A number of gully fields are visible on the top and base surfaces of the Fuji–Einstein system (Figs. 4, 5, 14) and also along the boundaries between delta lobes. Individual gullies range from less than 80 m to over 500 m wide (Fig. 15) and are up to 50 ms TWTT (~ 40 m) deep. The largest gullies are more than 25 km in length; they commonly terminate in areas 2–5 km wide consisting of high-amplitude reflections. In contrast, many smaller gullies do not have associated high-amplitude zones at their terminations; instead they gradually die out below seismic resolution where the slope gradient decreases, with no appreciable increase in amplitude.

Upslope, each gully field appears to be sourced from a single coeval shelf-edge delta lobe, with gully fields forming both on the downlap surface of the prograding deltaic clinoforms and on the clinoforms themselves. The stratigraphic position and location of gullies can be used to predict upslope shifts in delta position.

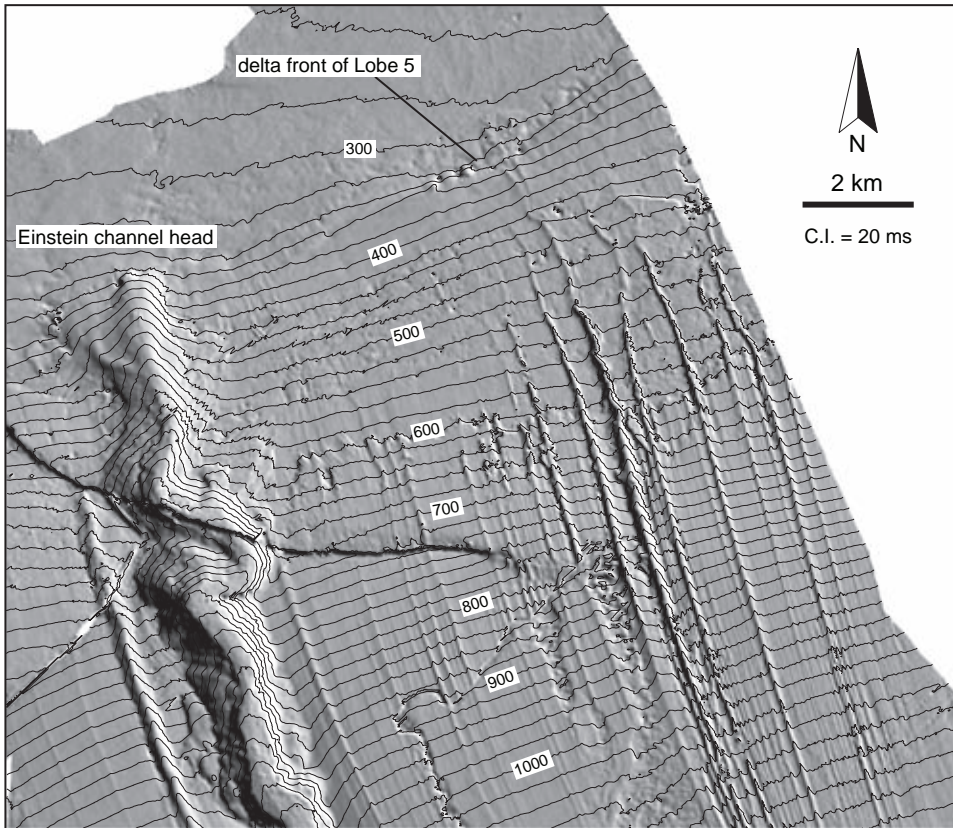F<small>IG.</small> 14.—Detail of shaded relief map of top Fuji–Einstein surface, showing the Einstein channel head and the youngest set of slope gullies that are linked to delta lobes 4 and 5. Location of map is shown in Figure 4.
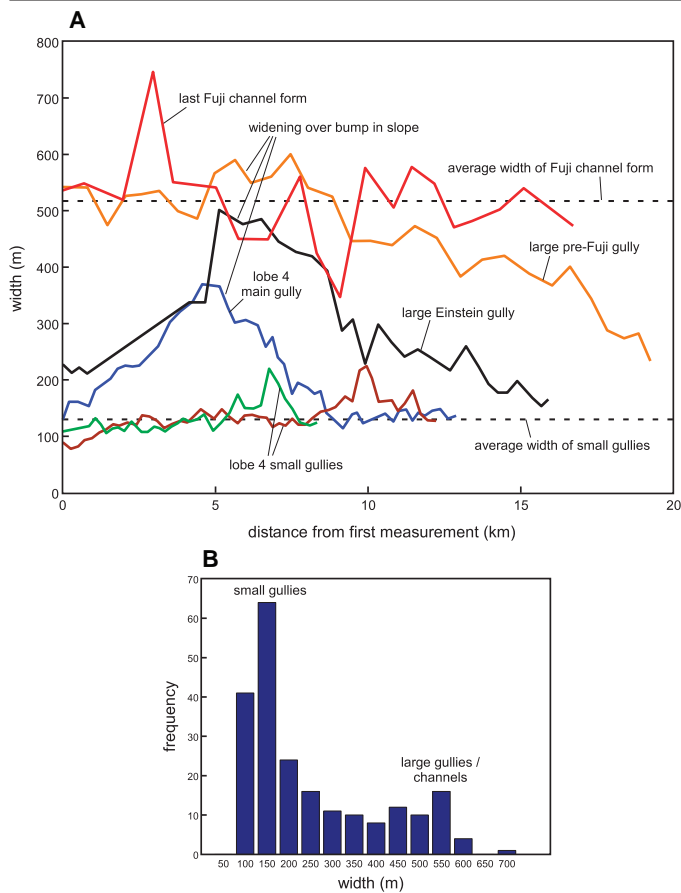
F<small>IG.</small> 15.—**A)** Widths of gullies and channel forms plotted against downdip distance. **B)** Histogram of measured gully and channel-form widths.

The connection between the delta top and the slope gullies is most obvious and best developed in the case of lobe 1. Channel-like features on the delta top directly link to a large gully (or small channel) on the upper slope (Fig. 13). A large gully field is present on the base Fuji–Einstein surface; they are clustered around Fuji channel and can be linked to lobe 2 (Fig. 5). A number of high-amplitude streaks are associated with these, suggesting a sand-rich source during lobe 2 deposition (Fig. 16).

Gullies are also present on the basal downlap surface of delta lobe 3; however, only the largest two of these gullies are visible on the top Fuji–Einstein surface, on the two sides of Einstein Channel (Fig. 14). The gully field seen to the east of Einstein Channel is sourced from lobe 5 (Fig. 14). Unlike on lobe 1 (Fig. 13), the connection between the delta-lobe top and the gullies is not fully developed; only subtle tributary networks starting at the offlap break and converging toward the gullies are apparent

FIG. 16.—Amplitude map of base Fuji–Einstein surface, draped over shaded relief map. Red colors correspond to high amplitudes, blue colors to low values. Seismic data courtesy of CGG Veritas.

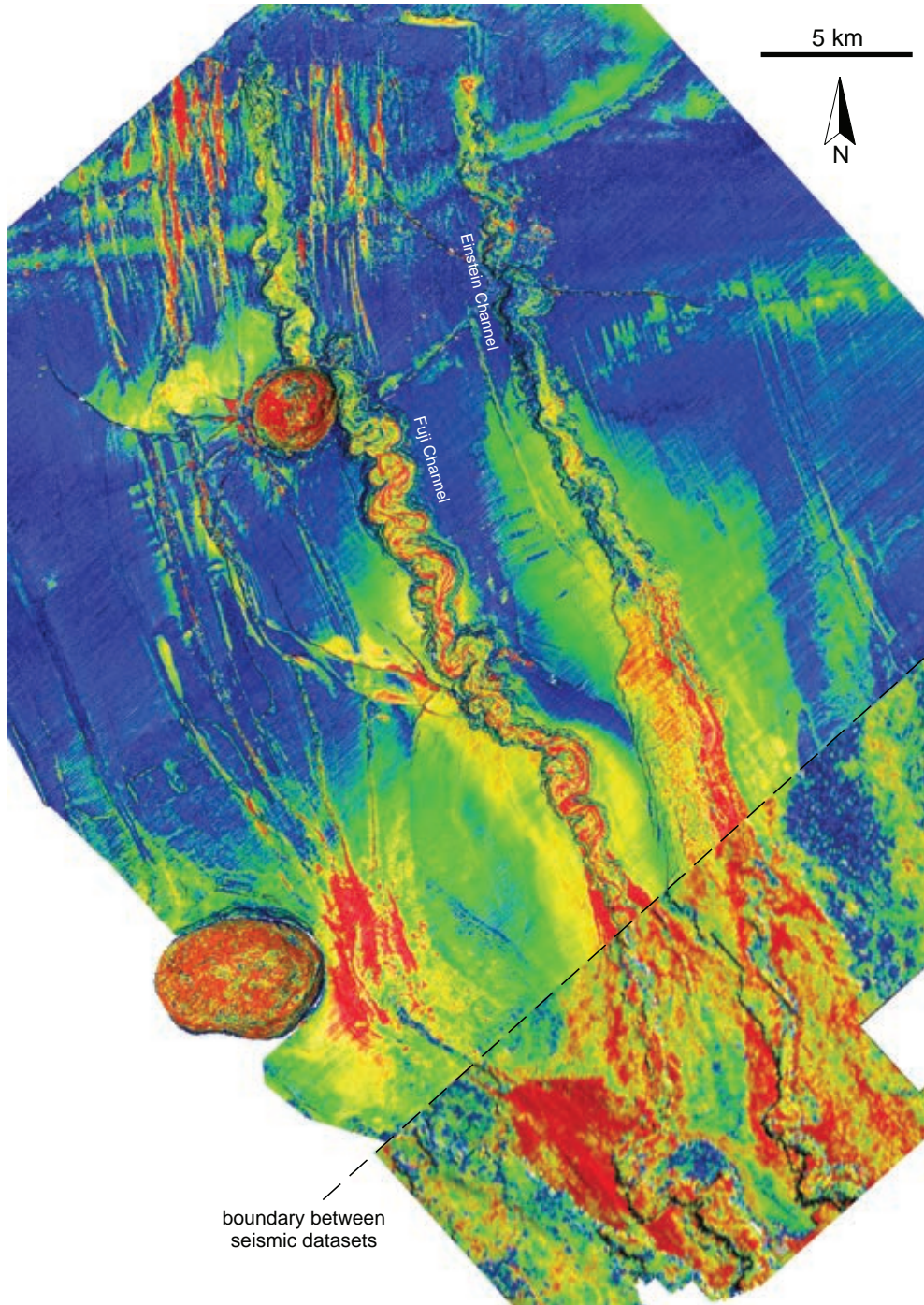(Fig. 14). The largest gully, in the center of the gully field, is linked with a circular area of deformation and/or erosion at the apex of the offlap break of the delta.

Interpretation.—

Our observations are consistent with the interpretation that these slope gullies are predecessors to the Fuji and Einstein channels (Posamentier, 2003; Faulkenberry, 2004). The gully field that links to lobe 5 represents an early stage of channel evolution, with the largest gully situated in the middle of the gully field, precisely downdip of the lobe apex (Fig. 14). If there had been enough time and sediment input for lobe 5 to develop into a significantly larger delta lobe, it is likely that this central gully would have evolved into a channel similar in size and character to Fuji and Einstein. A later stage of development is captured by the gullies related to lobe 3 and Einstein Channel: the two largest gullies are flanking the channel in the center, suggesting that the channel evolved from the central gully. Evidence for sinuous channels developing from smaller straight slope gullies has been described by Gee and Gawthorpe (2007). The links between individual delta lobes and slope gully fields appear to be strong in this case, in contrast with gullies and channels on the Brunei slope (Straub et al., this volume).

Slope Channels

Description.—

Compared to channel–levee systems of large and long-lived deltas (e.g., Indus, Zaire, Amazon, Rhone), the Fuji and Einstein channels are much smaller (Deptuck et al., 2003). Still, they are relatively large systems: the average distance between the levee crests of Fuji exceeds 2000 m, and the average total channel relief (from the averaged levee crest to the channel base) is 166 ms TWTT (~ 150 m).

Link to Delta Lobes.—The two channels link to lobes 2 and 3 of the updip shelf-edge delta through two canyon-like features (Figs. 8, 10, 11, 12, 17). These incisions extend updip into the proximal parts of the delta, where they terminate against the Fuji–Einstein top surface. The incisions cannot be linked to any
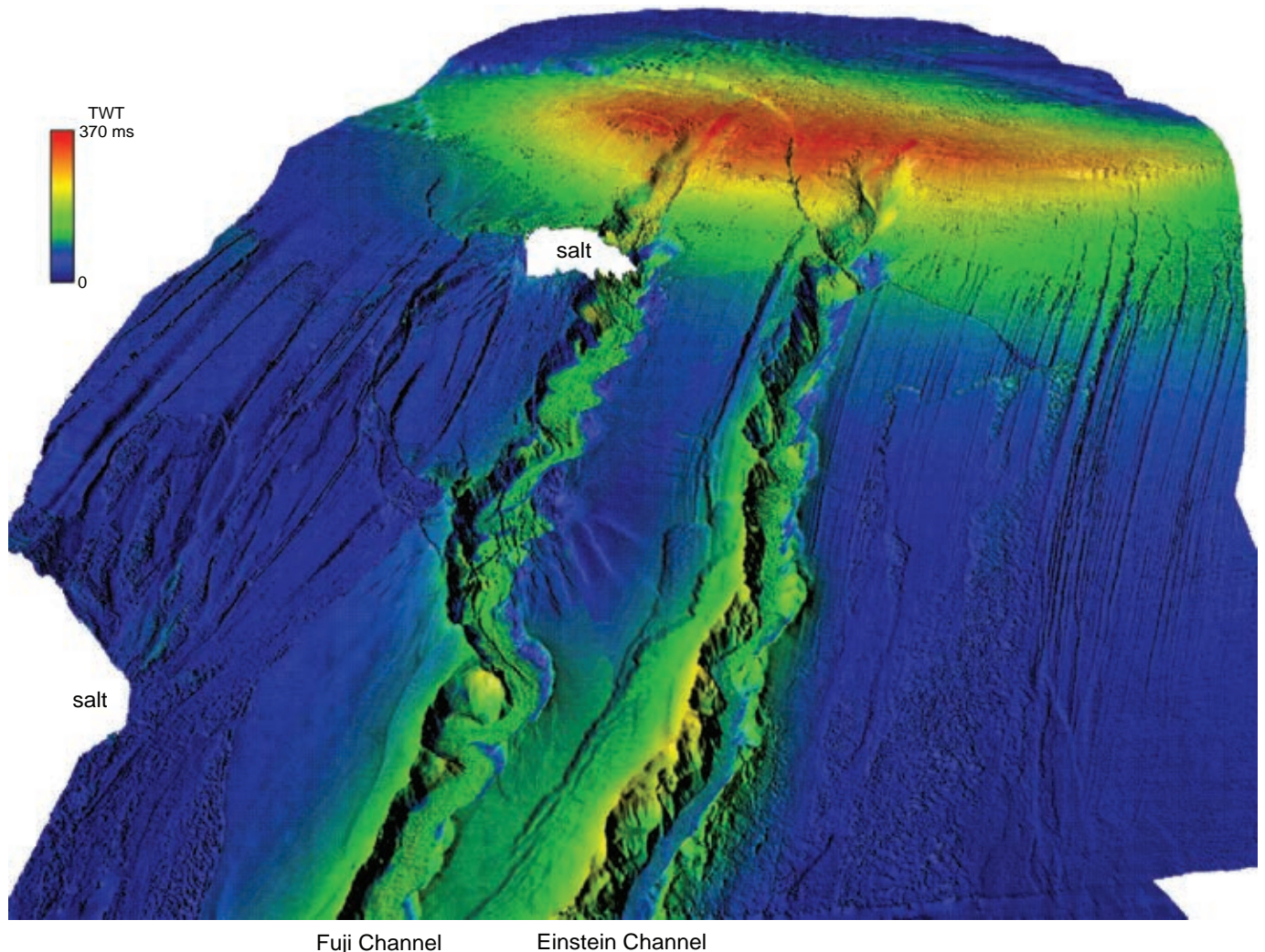

Fuji Channel   Einstein Channel

FIG. 17.—Three-dimensional view of top Fuji–Einstein surface, colored with thickness of the Fuji–Einstein system.

incision farther updip on the shelf, at least not within the resolution of the available seismic data. Farther downdip, the bases of the incisions reach the basal downlap surface of the delta and incise the slope as well, and become the basal erosional surfaces of the slope channels (Fig. 5). The depth of incision is about 250 m at the thickest part of the delta; the maximum width is about 2 km. The incisions appear to form two large erosional surfaces separating older deltaic clinoforms from a younger canyon fill. However, closer inspection shows that there are multiple erosional surfaces and the canyon fill consists of clinoforms that can be traced locally into clinoforms outside of the incision. Although there are uncertainties about how exactly the canyon-fill deposits correlate with out-of-canyon strata, lower parts of the canyon fills seem to be coeval with the progradation of lobes 2 and 3 (Fig. 18). The upper parts of the canyon fills are related to smaller-scale, late-stage deltas that formed during deposition of lobes 4 and 5 (Figs. 11, 12, 18; Table 1) and fill the proximal parts of the slope channels (see also Posamentier, 2003; Winker and Shipp, 2003). In the Fuji channel, clinoforms of this late-stage delta seem to be coeval with the uppermost part of the channel fill that is continuous throughout the upper slope (Fig. 19). The clinoforms of the early delta (which is part of lobe 2) and those of the late channel-head delta correlate downdip in the channel to a more disorganized seismic facies that corresponds to channel-fill turbidites and potentially slump and debris-flow deposits (Fig. 19).

Slope Expression.—On the slope, high-amplitude reflections (HARs) at the basal and axial parts that give way to generally low-amplitude seismic events within the levees characterize both channels (Figs. 16, 20). Multiple high-amplitude threaded pat-terns reflecting lateral and downstream migration of individual channel forms characterize the basal erosional surface (Fig. 21). Each of these narrow threads is ~ 100 m wide and represents the locally preserved bases of the channels, whose actual channel widths are more than 500 m at the top (Fig. 15A). This is consistent with the observation that the high-backscatter channel thread representing the thalweg of the Amazon Channel is two to three times narrower than the actual bankfull width (Pirmez and Imran, 2003).

Individual channel forms in Fuji and Einstein channel belts have dimensions similar to those of the largest slope gullies (Fig. 15). The two important differences are: (1) Fuji and Einstein have significant levees, whereas slope gullies lack overbank deposits that are resolvable with the available seismic data; and (2) unlike the linear slope gullies, Fuji and Einstein developed relatively high sinuosities. Because it appears that channel-belt widening occurs mainly through channel migration and the related increase in sinuosity, lower-sinuosity areas are characterized by narrower channel belts.

Lithologic Calibration.—The three research wells drilled in the Einstein channel–levee and an additional industry well targeting deeper objectives show that the high-amplitude reflections at the channel bases correspond to coarser-grained deposits, whereas the levees consist predominantly of mudstones (Fig. 20). The high-amplitude channel-base facies has a net-to-gross of 24%; well E penetrates an ~ 5-m-thick unit of pebbly sand at the base of Einstein (Fig. 20; Hackbarth and Shew, 1994). Sidewall cores from an exploration well (VK 783 #1) that penetrate the axis of the Einstein channel farther updip (Fig. 4) also contain sand and gravel; wire-line logs indicated 18 m net sand with some thin shale interbeds.

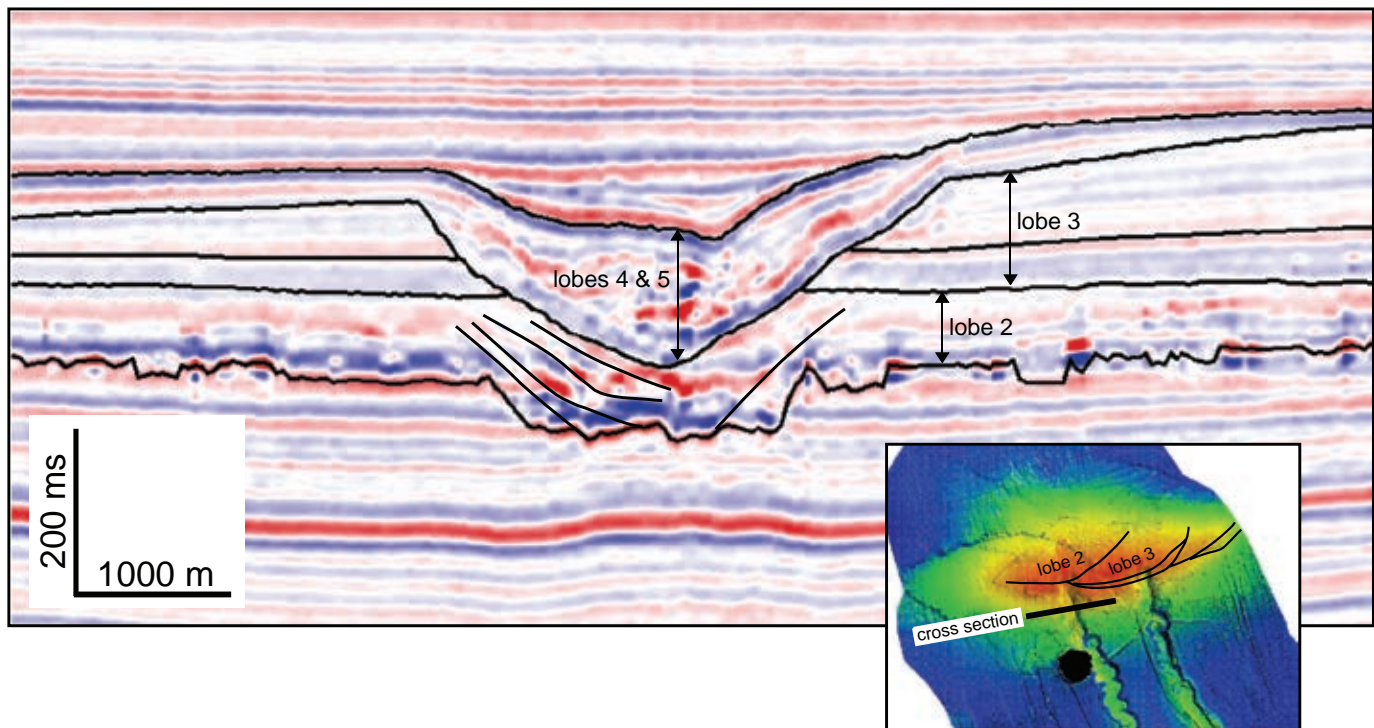FIG. 18.—Cross section showing part of the Fuji–Einstein prodelta cut by the Fuji canyon head. Stratigraphic relationships suggest (1) that early evolution of the channel was coeval with Lobe 2 progradation; and (2) the channel was reactivated during later stages of delta evolution, after abandonment of both the Fuji and Einstein delta lobes. Location of cross section is shown in Figure 4. Seismic data courtesy of CGG Veritas.

TABLE 1.—Summary of events affecting Fuji and Einstein channels during the deposition of different delta lobes

Delta lobe	Events affecting Fuji Channel	Events affecting Einstein Channel
Lobe 1	N/A	N/A
Lobe 2	gully field; central gully develops into Fuji Channel	N/A
Lobe 3	abandoned; partially filling with mud belt of lobe 3	gully field; central gully develops into Einstein Channel
Lobe 4	small channel-head delta, late channel fill	abandoned; partially filling with sediment from lobe 4
Lobe 5	abandoned	abandoned

Interpretation.—

It appears that both the Fuji and Einstein channel belts formed as the two channels migrated laterally and downstream while eroding into the substrate at the same time. The combination of channel migration and incision resulted in significant widening of the channel belt. This explains the 1700 m average erosional width of the Fuji channel, more than three times the average width of the last channel form. The youngest channel form is the most mappable because earlier channels have been partially removed by erosion. The basal erosional surface is a composite surface that never existed as such at any point in time, although it is the most obvious mappable seismostratigraphic event. The high-amplitude channel-base threads on this surface suggest a regular and relatively continuous channel migration, and there is no evidence of repeated large-scale filling and reincision of the channels. High-
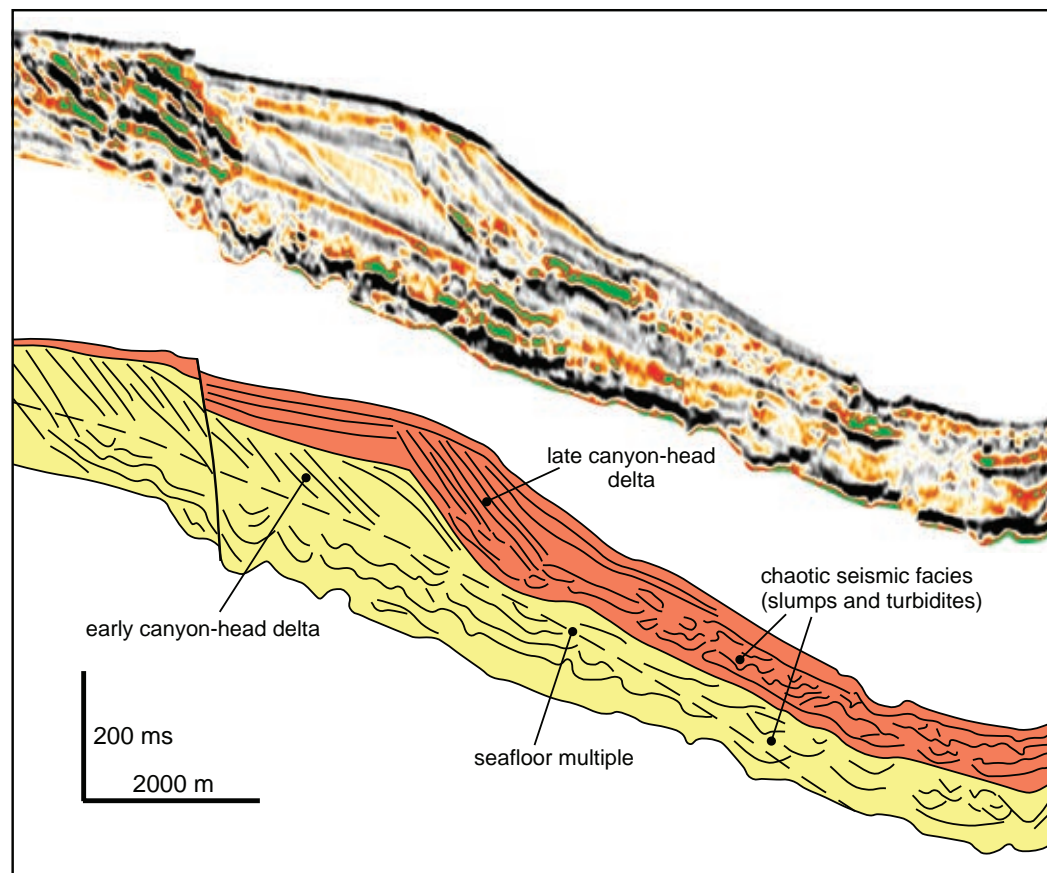

FIG. 19.—Dip section along the Fuji canyon head, showing relationships between canyon-head deltas and the more chaotic channel fill. Location of cross section is shown in Figure 4. Seismic data courtesy of CGG Veritas.
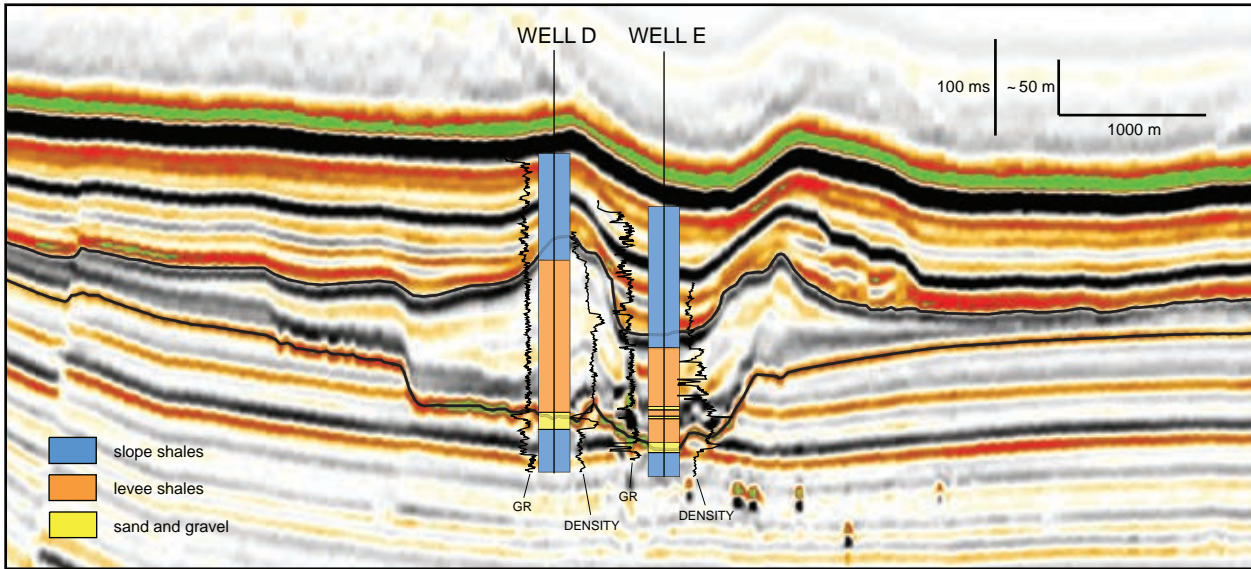
FIG. 20.—Seismic cross section with research wells D and E, drilled into the axis and levee of Einstein channel. Well data from Hackbarth and Shew (1994). Location of cross section is shown in Figure 4. Seismic data courtesy of CGG Veritas.
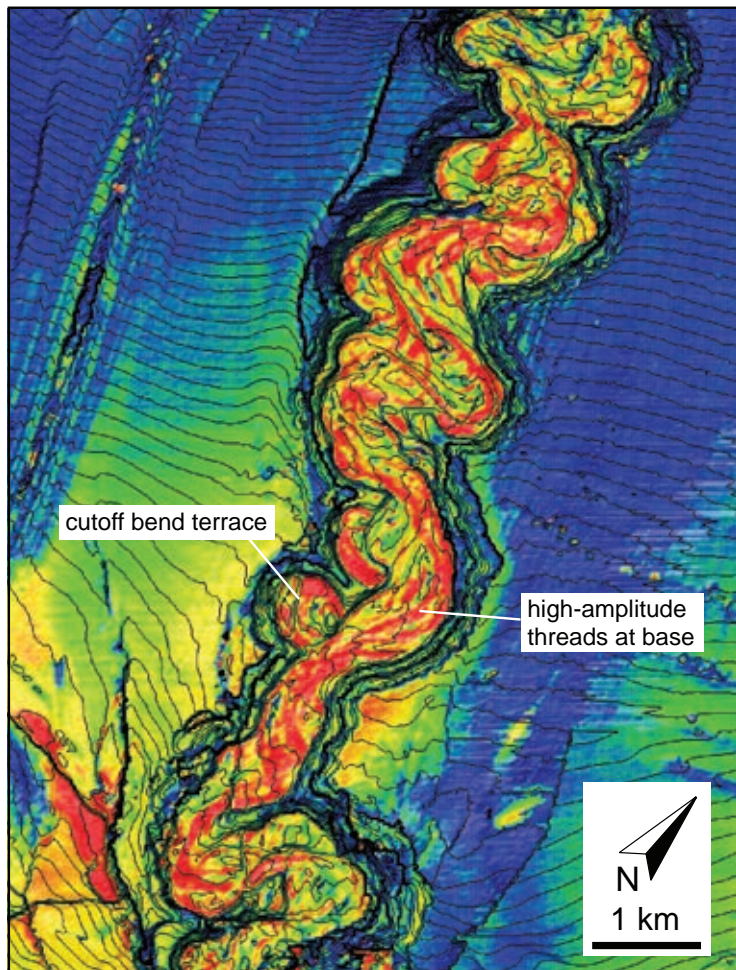

FIG. 21.—Detail of base Fuji channel (amplitude draped over shaded relief map).

quality seismic datasets increasingly suggest that this style of submarine slope-channel evolution is more common than previously thought (e.g., Abreu et al., 2003; Schwenk et al., 2005; Sylvester et al., in press).

The fact that coarse-grained sediment is restricted to the basal part of the channels is consistent with the distribution of the high-amplitude seismic facies. The actual relief at time of deposition was much larger (~ 150 m) than the thickness of deposited sand (15–20 m), and therefore one has to be careful when interpreting the paleo-relief of channels from well logs and outcrops.

In contrast with channel–levee systems of large submarine fans, which are largely unaffected by local deformation of the slope (e.g., Pirmez and Flood, 1995; Babonneau et al., 2002), the history of Fuji and Einstein channels is complicated by areas of local uplift or subsidence associated with salt movement or large counterregional faults (Figs. 3, 4, 16). The along-channel section of Fuji (Fig. 22) suggests that uplift along the upper reaches of this channel was active during and after channel development. The slope channels were in general able to outpace contemporaneous slope deformation and created a concave-upward profile that smooths out the convex-upward parts of the upper slope (green line in Figure 22). Estimated total erosion by the Fuji channel is more than 200 m in places with significant uplift. In both channel systems, the top of the channel fill and the averaged top of the levees are roughly parallel to the channel base; this results in thicker levees where the depth of incision is small and thinner levees where the depth of incision is larger (Fig. 22). These relationships are similar to those observed on the Benin-minor system of the western Niger Delta (Deptuck et al., this volume).

An important question regarding the origin of slope channels is whether they result from headward erosion of slide scars forming on the slope that fortuitously capture gravity flows (e.g., Farre et al., 1983) or from progressive widening of gullies sourced by deltas. Evi-

dence from the northeastern Gulf of Mexico favors the latter model, although headward erosion played a significant role in widening the channels and eroding deeply into the delta lobes, in a manner similar to the model of Pratson and Coakley (1996). The delta lobes seem to determine the locations of the linked slope channels, as opposed to erosional features on the upper slope influencing the positions of new delta lobes.

The stratigraphic relationships observed in delta lobe 1 suggest a direct connection between the upper-slope gullies or channels and the larger fluvial channels (Fig. 13) and are similar to those observed on the Fraser River delta in British Columbia (Hart et al., 1992; Hill et al., 2008) and at the mouth of the Puyallup River in Washington state (Mitchell, 2005).

Slope Aprons

Description.—

A number of slope aprons, that is, mostly lobate, laterally extensive deposits (Prather et al., this volume; termed "frontal splays" in Posamentier, 2003), are present on the slope in the study area. They are characterized by relatively high amplitudes within a single seismic loop (Fig. 16). Typically, they link to the largest gullies or to the slope channels, have a well-defined updip boundary, and fade out gradually in a downdip direction (Fig. 16). Their width does not exceed 8 km; their maximum visible downslope dimension is 12 km.

Research well D penetrated the updip part of the slope apron sourced by Einstein Channel, and found that the relatively high amplitudes correspond to an ~ 8-m-thick sandy unit. At this location the Einstein channel is filling a preexisting translational slide scar (Hackbarth and Shew, 1994). Parts of the slide scar are characterized by an irregular topography created by slide blocks that moved over short distances from the scarp.

Interpretation.—

Posamentier (2003) interprets the submarine aprons linked to the Fuji and Einstein channels as frontal splays deposited by the channels during the "middle lowstand". Later, during the late lowstand, muddier flows resulted in significant extension of the channels across the frontal splays. In a third stage, further decrease of the sand–mud ratio within the flows led to the incision of the channels.

A decreasing sand content of sediment gravity flows is consistent with the lithologies penetrated by the three research wells (Fig. 20). However, the change from apron deposition to incising bypass channels is an expected result of adjustment to a smoother equilibrium profile across a step, and there is no need to invoke changing flow composition. The aprons in the study area are associated with areas of lower gradients on the slope. The extents of the aprons associated with Fuji and Einstein channels are centered on the locations of gradient change from higher to lower slope, on the surface that predated channel development and incision (Fig. 22). These aprons must have been early features deposited by the large gullies that later developed into Fuji and Einstein channels. They are analogous to the "transient fans" of Adeogba et al. (2005) and to the "perched aprons" of Deptuck et al. (this volume) and Prather et al. (this volume).

In contrast with the aprons associated with the Fuji and Einstein channels, which were incised throughout their entire length, the apron deposited around the Pascagoula salt dome (Figs. 16, 23A) represents an earlier stage of apron development, and the incision is restricted to a tributary network of gullies on the downdip side of the apron. These tributaries converge to form two large gullies farther down the slope. Several turbidite reservoirs in the northeastern Gulf of Mexico, found at deeper levels with lower seismic resolution, have similar patterns of deposition and erosion. For example, the amplitude map of the J reservoir of the Ram Powell field (e.g., Clemenceau, 1995) is likely to represent a submarine apron dissected by one major bypass channel (Fig. 23B).

Relatively high amplitudes and patterns suggestive of submarine apron deposition are also present on the hanging walls of the counterregional faults located downdip of lobe 2 (Figs. 16, 24). Updip knickpoint migration due to headward erosion occurs across a relay ramp between two faults.
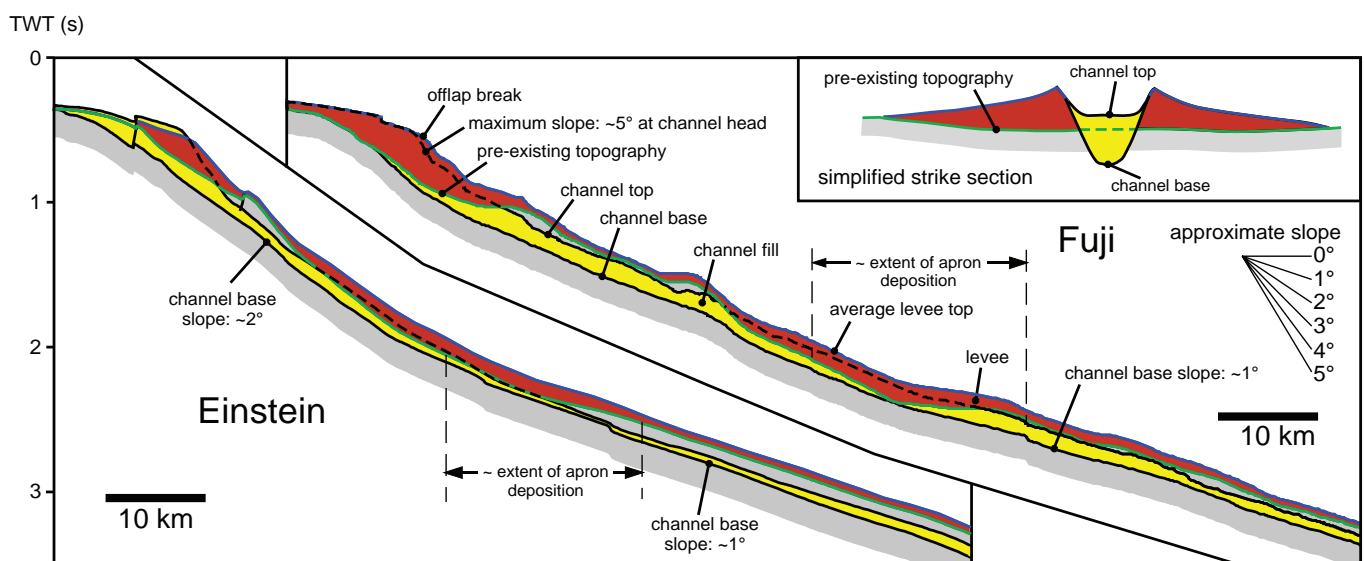

FIG. 22.—Along-channel profiles of Fuji and Einstein channels, showing the erosional channel base, the channel-fill top, the preexisting topography (green line; interpolated from the sides across the channel cuts), and the average levee top (blue line).
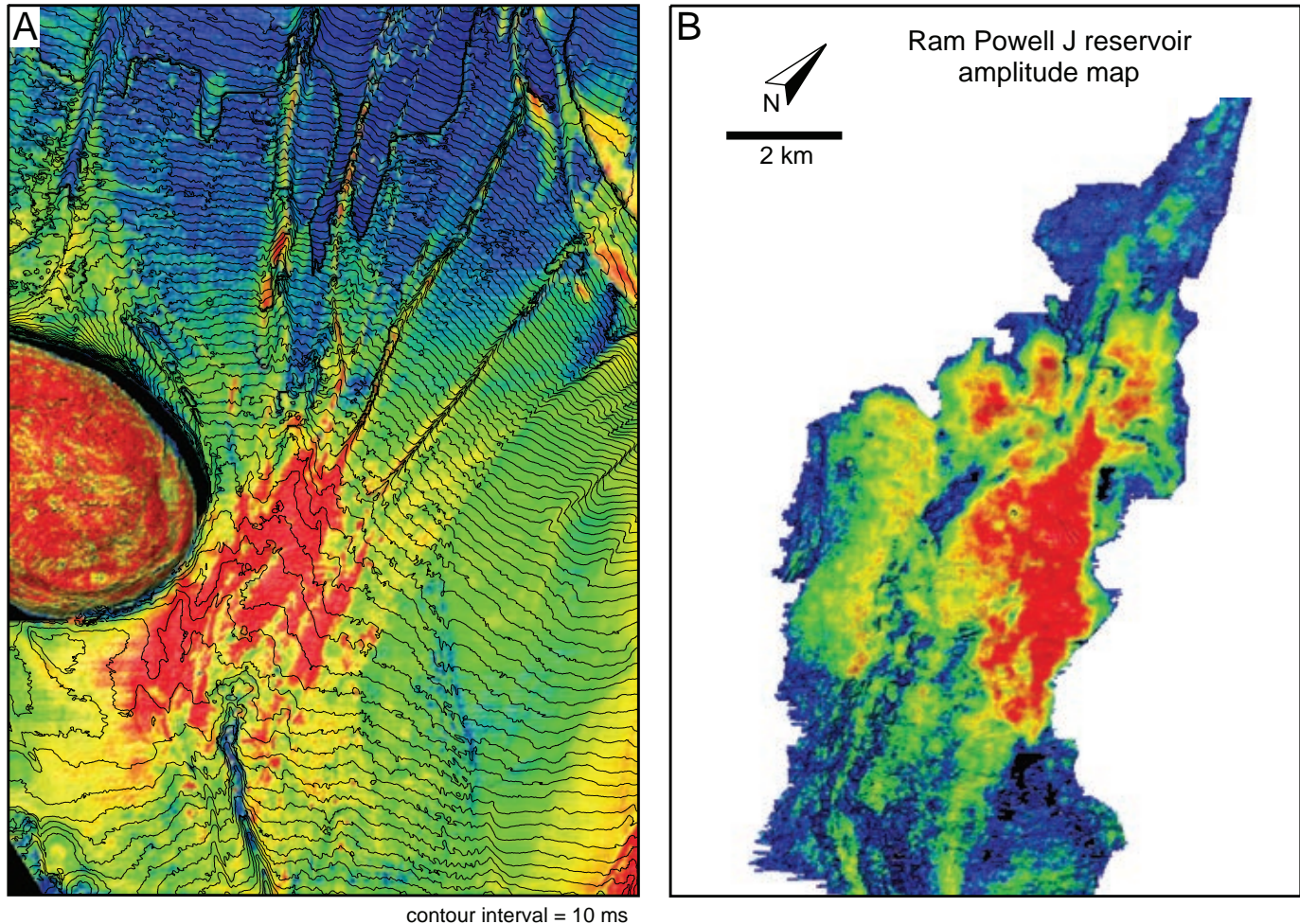
contour interval = 10 ms

FIG. 23.—**A)** Amplitude map of slope apron deposited next to Pascagoula Dome, sourced by multiple gullies that are linked to the Fuji delta lobe (Fig. 16). **B)** Amplitude map of Ram Powell J reservoir, showing patterns similar to those in Part A, but at lower seismic resolution. Both maps have the same scale. Seismic data courtesy of CGG Veritas.

Mud Belts

Description.—

The intervals above and below the top and base Fuji–Einstein surfaces consist of several continuous seismic reflections that onlap the upper slope in the updip direction and terminate through downlap in the downdip direction. The seismic units defined by these terminations form along-slope ridges that are extensions of adjacent SEDs. Where penetrated by wells, these seismic units consist of shale (e.g., Fig. 20) and are referred to here as mud belts. A fine-grained lithology is also consistent with the continuity, amplitude, and draping nature of the seismic reflections. In most cross sections, the maximum thickness is far out on the upper slope, where they form large wedges. If followed in the updip direction, the reflections onlap the steeply dipping clinoforms of a shelf-edge delta (Fig. 25); toward the basin, the wedges thin more gradually and are interbedded with and replaced by chaotic seismic facies, suggestive of mass-transport complexes (MTCs). In cases where the basinward side of the wedge is steeper, the reflections may look like large clinoforms.

The mud belt immediately above the Fuji–Einstein system forms an elongated wedge that is parallel to the slope and is linked to a shelf-edge delta located to the west of the Fuji–Einstein delta (Fig. 26). The maximum thickness of the delta exceeds 300 m; the wedge gradually thins from ~ 160 m near the delta to ~ 100 m in the area east of Fuji channel. Significant thickening occurs where the wedge is filling the Einstein and Fuji channels. The mud belt below the Fuji–Einstein system (Fig. 27), located in a section with undulating reflections, is also linked to a delta. In this case the mud belt thickens towards the east, where there are several vertically stacked shelf-edge deltas (Figs. 25, 27). The most basinward parts of some mud belts are characterized by small-amplitude crenulations of the seismic reflections (Fig. 27). They have an average wavelength of 480 m (based on 64 measurements). Their amplitude is difficult to estimate with the resolution of the available seismic data, but it seems that in general it is less than 10 m.

The seismic geometries illustrated here suggest that mud belts build up most of the upper slope in the northeastern Gulf of Mexico (Fig. 28).
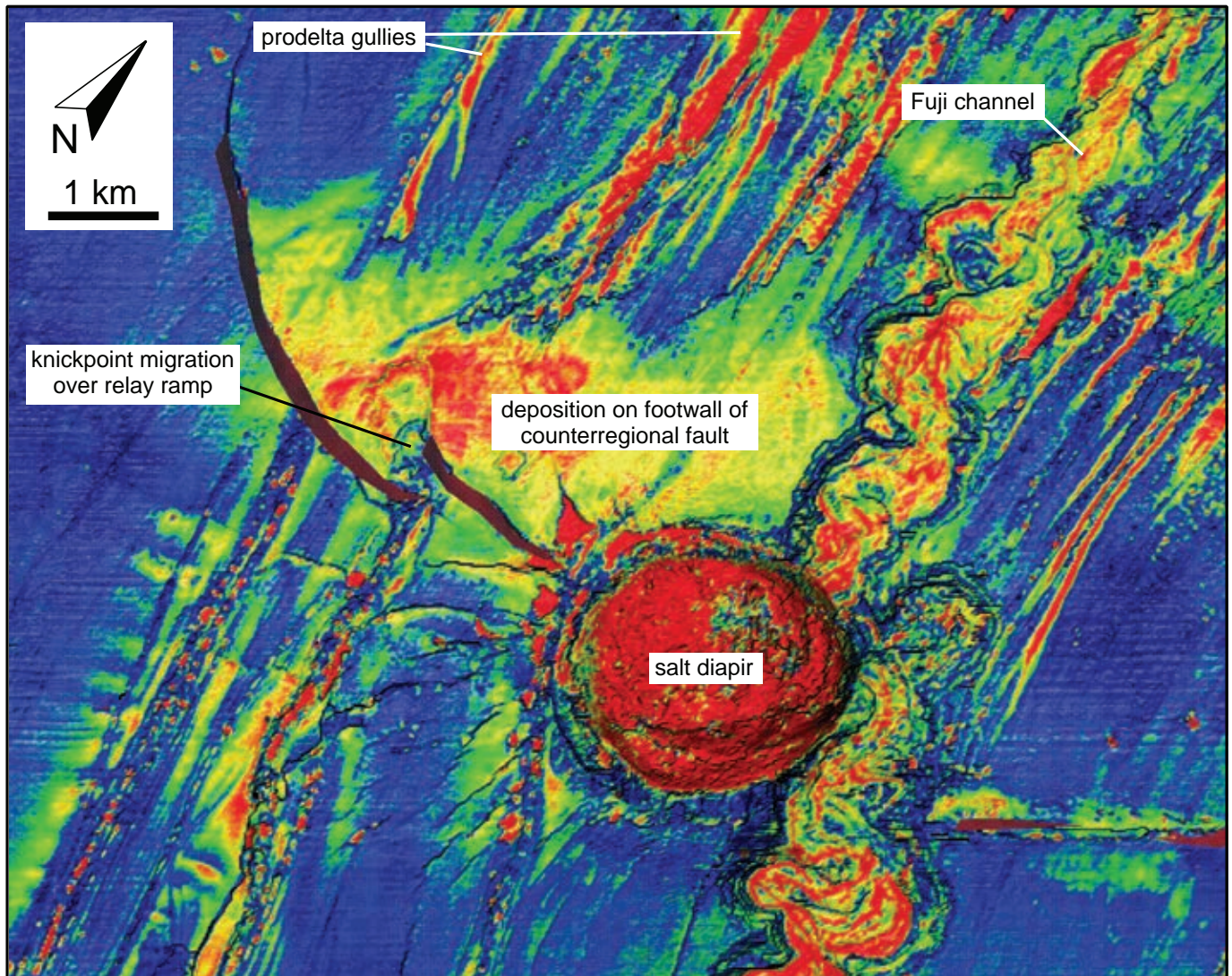
Fig. 24.—Detail of amplitude map of base Fuji–Einstein surface. Slope aprons are deposited on the footwalls of counterregional faults; bypassing flows caused knickpoint migration across relay ramp between two faults. Seismic data courtesy of CGG Veritas.

Interpretation.—

Delta-related muddy wedges and clinoforms have been described from numerous modern shallow marine settings (e.g., Cattaneo et al., 2003; Kuehl et al., 1997; Nittrouer et al., 1986), but their importance in the geologic record and their significance for facies models and sequence stratigraphy only recently started to be recognized (Fraticelli and Anderson, 2003; Vakarelov and Bhattacharya, 2004; Vakarelov, 2006). In many deltas, a significant part of the fine-grained sediment is transported in a longshore direction, resulting in elongated wedges that can extend over tens of kilometers from the deltaic source. Although the upper-slope wedges in Figure 24 are similar in geometry to the "healing-phase" deposits of Posamentier and Allen (1993)—sigmoidal reflections interpreted as parts of the transgressive systems tract — in the study area every mud belt seems to be linked to an out-of-plane shelf-edge delta, probably deposited during a sea-level lowstand. Fraticelli and Anderson (2003) described similar "healing wedge" deposits from the Brazos deltaic system in the west-ern Gulf of Mexico and suggested that their deposition is not restricted to a specific sea-level position; rather, they can form as long as there is a shelf-edge delta.

The small-amplitude undulations visible on some mud belts are likely to be sediment waves, which are common features on levees of submarine channels and on sediment drifts deposited by contour currents. Similar structures have been described in other prodelta settings as well (Aksu and Piper, 1983; Correggiari et al., 2001; Cattaneo et al., 2004; Trincardi and Normark, 1988). Their origin is not entirely clear, but the most widely accepted idea is that sediment waves form in a manner comparable to antidunes, under nearly stationary internal waves within dilute turbidity currents or contour currents, and they usually migrate updip (Normark et al., 1980; Normark et al., 2002). Compared to other sediment-wave fields, these bedforms are among the smallest. The slope-parallel orientation of the wave crests suggests that they were gravity currents, not contour currents, and hence they must have been sourced from the river that also deposited the mud belt.
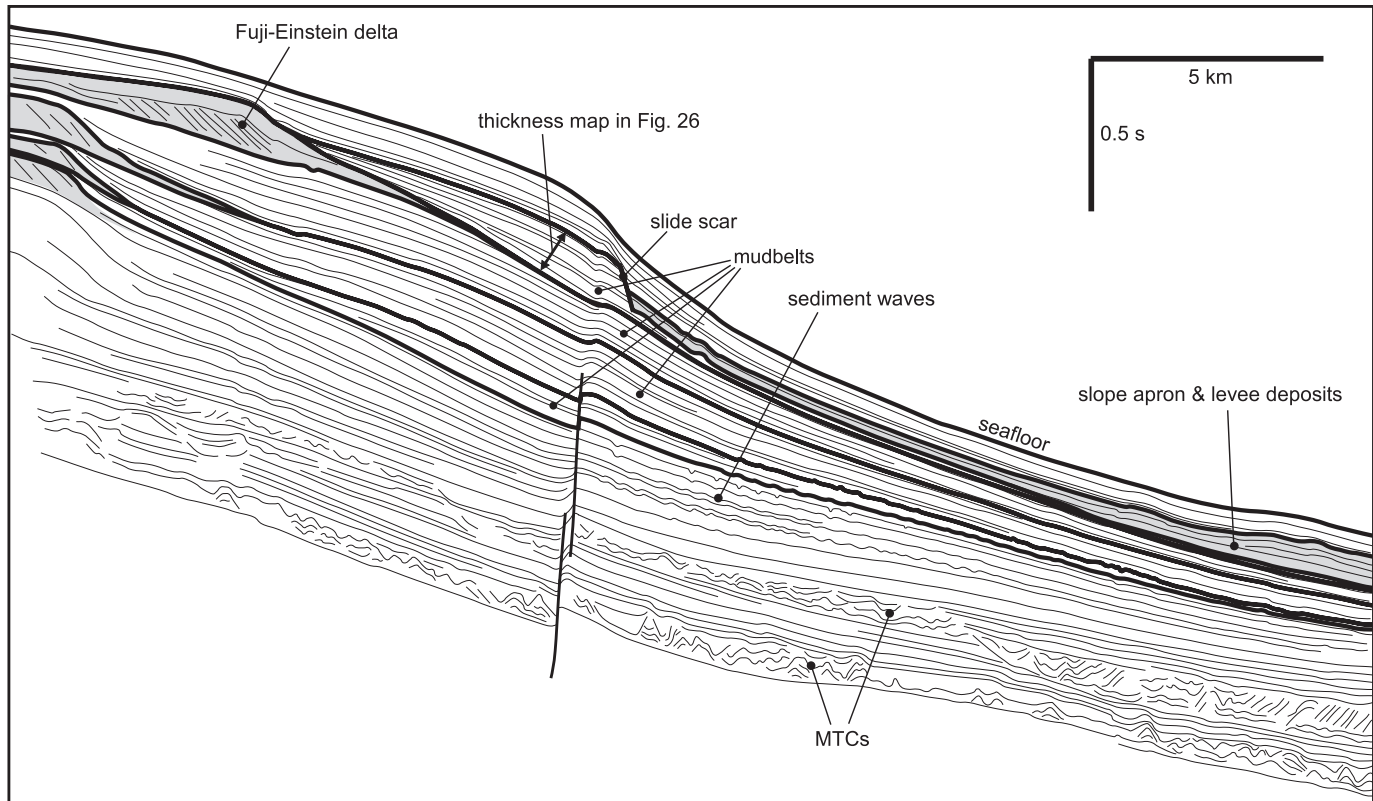
F<small>IG.</small> 25.—Dip section across eastern part of Fuji–Einstein system. Several shelf-edge deltas and upper-slope mud belts can be seen in such dip sections. Location of cross section is shown in Figure 4.

DISCUSSION

Sediment Transfer from Fluvial to Submarine Settings

The seismic structure of the Fuji–Einstein system suggests that sediment deposition and transport on the slope was at least partially coeval with delta progradation. The question arises: what was the dominant process for sediment transfer from the river to the turbidity currents on the slope? Although direct hyperpycnal flows are unlikely to occur at the mouths of rivers like the ones feeding the deltas in the northeastern Gulf of Mexico (Mulder and Syvitski, 1995), it is possible that convective instabilities converted the hypopycnal plume into a gravity current (Parsons et al., 2001). Alternatively, these currents originated as wave-supported suspensions forming on the outermost shelf and upper slope (e.g., Hill et al., 2007). Both hypopycnal plumes and wave-supported gravity currents would have generated relatively fine-grained, dilute, unchannelized turbidity currents with large lateral extents. Such currents could have formed both the sediment waves and the gully fields characteristic of early delta-lobe development.

The seismic resolution is not high enough to determine unequivocally the nature of the linkage between delta distributary channels and slope gullies or channels. However, the evolution from multiple smaller gullies to a single larger central slope channel either parallels a similar trend from multiple distributaries to a single channel in the fluvial system, or it marks the change from slope gullies disconnected from the fluvial system to a more direct connection with a single dominant fluvial channel. Evidence for wave-dominated lobes (Fig.

12) and for early slope gullies that begin below the shelf edge (Fig. 14) favor the latter interpretation. The change from the gully field to a single channel must correspond to a change from laterally extensive turbidity currents to more channelized and probably more sand-rich flows. These must have originated in the canyon heads (Figs. 17, 22), where slopes were the steepest and sand was available.

Implications for Sequence Stratigraphic Models and Sand Transfer to the Deep Sea

In section 1 of Figure 8, sigmoidal clinoforms of lobe 3 onlap onto the foresets of the lobe 2. In sequence stratigraphic models, this relationship would correspond either to the contact between the highstand systems tract and the lowstand systems tract, or to the transition from the falling-stage systems tract to the lowstand systems tract. This geometry is also reminiscent of the "healing wedge" of Posamentier and Allen (1993), which is interpreted as fine-grained sediments deposited during transgression. However, three-dimensional mapping of the delta lobes shows that this onlapping sigmoidal unit is the western extension of the lobe 3 (Figure 8C; see also Winker, 1993a, 1993b), and therefore is the result of delta-lobe switching rather than sea-level changes.

Sequence stratigraphic analysis of single dip sections in shelf-edge deltas can easily result in erroneous interpretations. Most individual dip sections through the Fuji–Einstein delta fail to capture the 3D delta geometries because significant parts of the stratigraphic history are missing from them. In conventional sequence stratigraphic diagrams, a lowstand wedge or a lowstand delta downlaps deep-water deposits on the slope and the
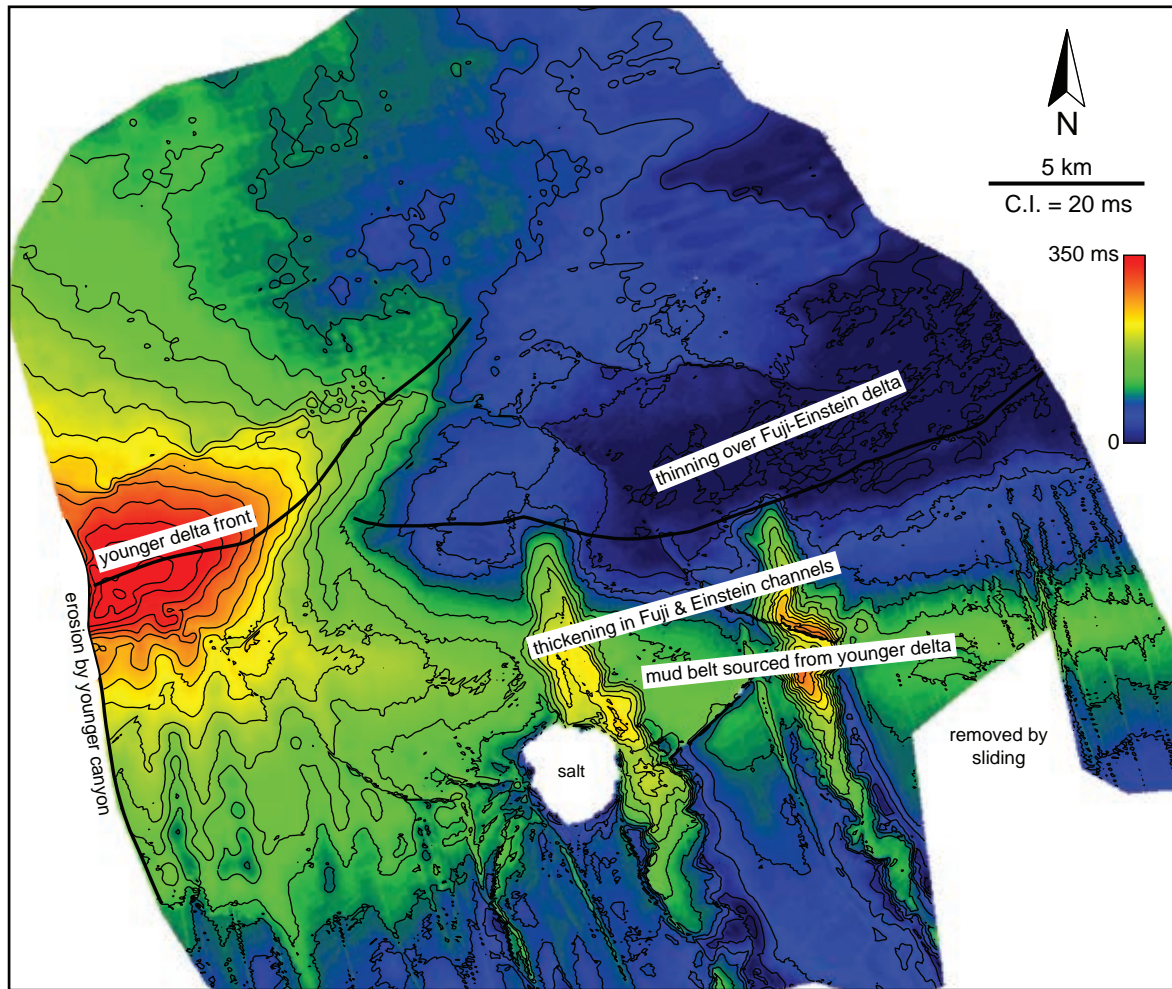
FIG. 26.—Thickness map of seismic unit overlying the Fuji–Einstein system (see Figure 25 for stratigraphic position). The elongated, slope-parallel wedge is a mud belt that is linked to a shelf-edge delta to the west of Fuji–Einstein.

basin floor (e.g., Posamentier et al., 1988; Myers and Milton, 1996; Catuneanu, 2006). Although clinoforms of the Fuji–Einstein shelf-edge delta also downlap the upper slope, the underlying sediments are usually not turbidites deposited earlier during the same sea-level cycle, but upper-slope deposits related to either a different lowstand or a different lobe of the same delta. The continental slope is tens of kilometers long in the northeastern Gulf of Mexico; no shelf-edge delta is able to prograde over such a distance. As a result, the sand-rich deltas and the related turbidite aprons and basin-floor fans are widely separated in space and are linked only by slope channels or canyons. At the resolution of the seismic data, the distal clinoforms of the shelf-edge delta are continuous and coeval with the levees of the slope channel (Figs. 11, 22); the submarine channel fills can also be traced into the deltaic clinoforms, with no intervening major discontinuity (Fig. 19). Downlap of prodelta clinoforms onto slope-apron turbidites is present only locally, where the aprons are close to the shelf edge (Fig. 8, section 1).

In sequence stratigraphic terminology, the Fuji–Einstein delta consists of a falling-stage systems tract (that includes lobes 1, 2, and most of lobe 3) and a lowstand systems tract (late lobe 3, with lobes 4 and 5). The Fuji and Einstein channel–levee systems and

the associated aprons and basin-floor fans are largely coeval with the falling-stage systems tract, whereas the lowstand systems tract is expressed on the slope as only (1) late-stage channel fills sourced by reactivated canyon-head deltas and (2) slope drapes extending from the prodelta clinoforms, dissected by gullies with no aprons at their terminations. This is consistent with a change to more mud-rich sediment gravity flows by late-lowstand time, as suggested by Posamentier (2003), but there is no evidence for late-stage incision of the Fuji and Einstein channels. Rather, the seismic data suggest that these late-lowstand flows must have been largely depositional within the channels.

This study suggests that maximum transfer of sand to the deep sea is characteristic of maximum progradation during forced regression. The forced regressive wedge forms the volumetrically most significant part of the delta, and it is relatively well preserved. Although the submarine channels incise deeply into the edge of the delta and probably were directly linked to fluvial channels, no incised valleys were eroded by fluvial systems on the delta top. In the study area, relatively large slope channels, submarine aprons, and basin-floor fans developed without significant fluvial erosion of the falling-stage delta, in contrast with the idea that widespread fluvial incision of the delta top is
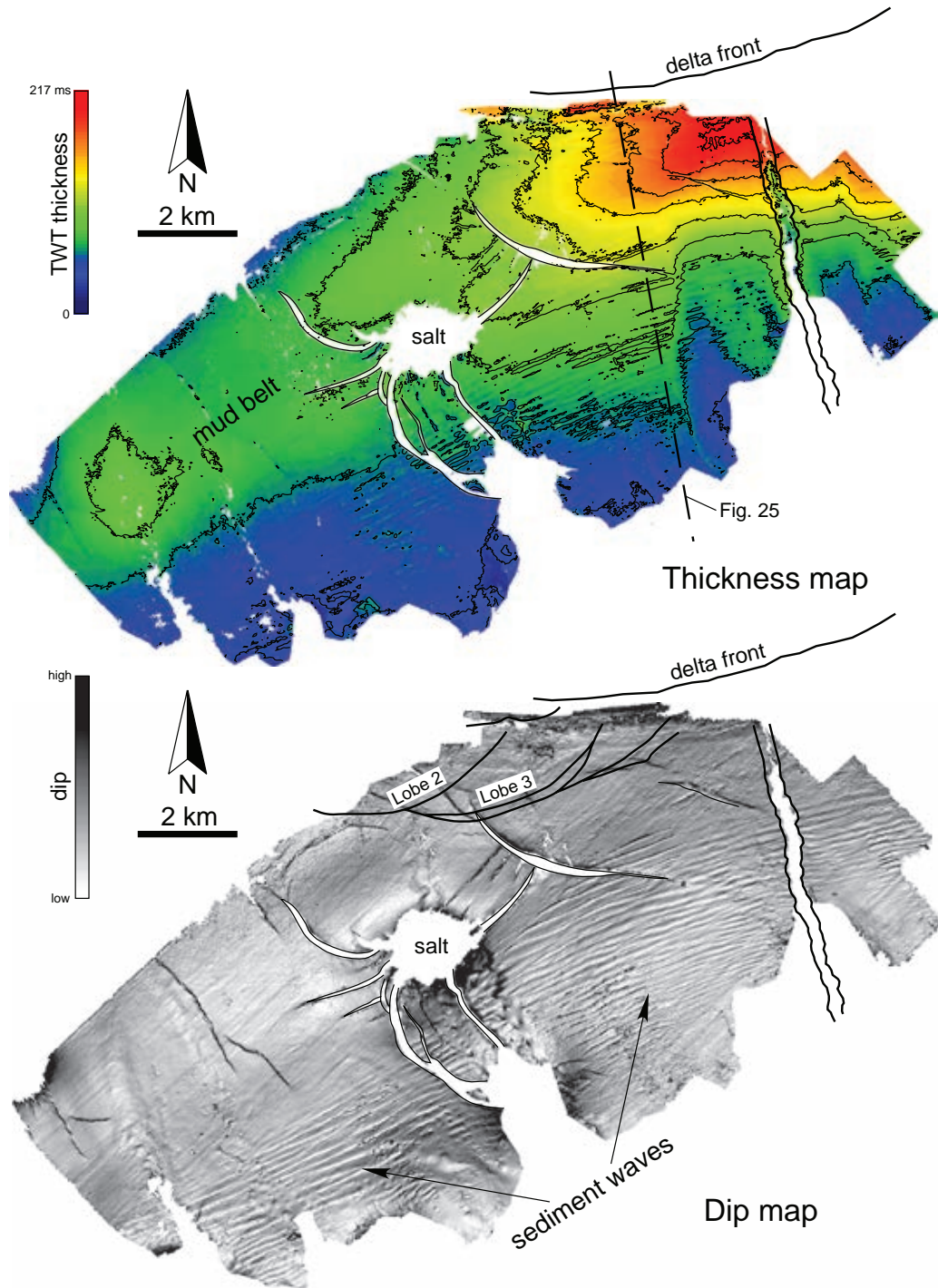
FIG. 27.—Thickness map and dip map of top surface of a seismic unit older than the Fuji–Einstein system. The thickness pattern is suggestive of a mud belt linked to a shelf-edge delta older than Fuji–Einstein. Seismic data courtesy of CGG Veritas.

necessary for significant sand transfer to the deep sea (e.g., Plink-Björklund and Steel, 2005; Porebski and Steel, 2003). Development of submarine channels did result in significant headward incision of delta lobes, but the sediment volume excavated and transferred to the deep sea in this fashion must have been only a fraction of the total quantity that reached the basin floor. Instead, the importance of these incisions lies in the establishment of a

direct link between the fluvial system and the submarine channels, facilitating the transfer of sediment directly to the deep sea, without significant storage time at the shelf edge. Linking the presence of sand in the deep sea to type I sequence boundaries on the shelf and cannibalization of falling-stage shelf-edge deltas assumes that sands must either form shelf-edge depocenters or accumulate predominantly on the basin floor. The Fuji–Einstein

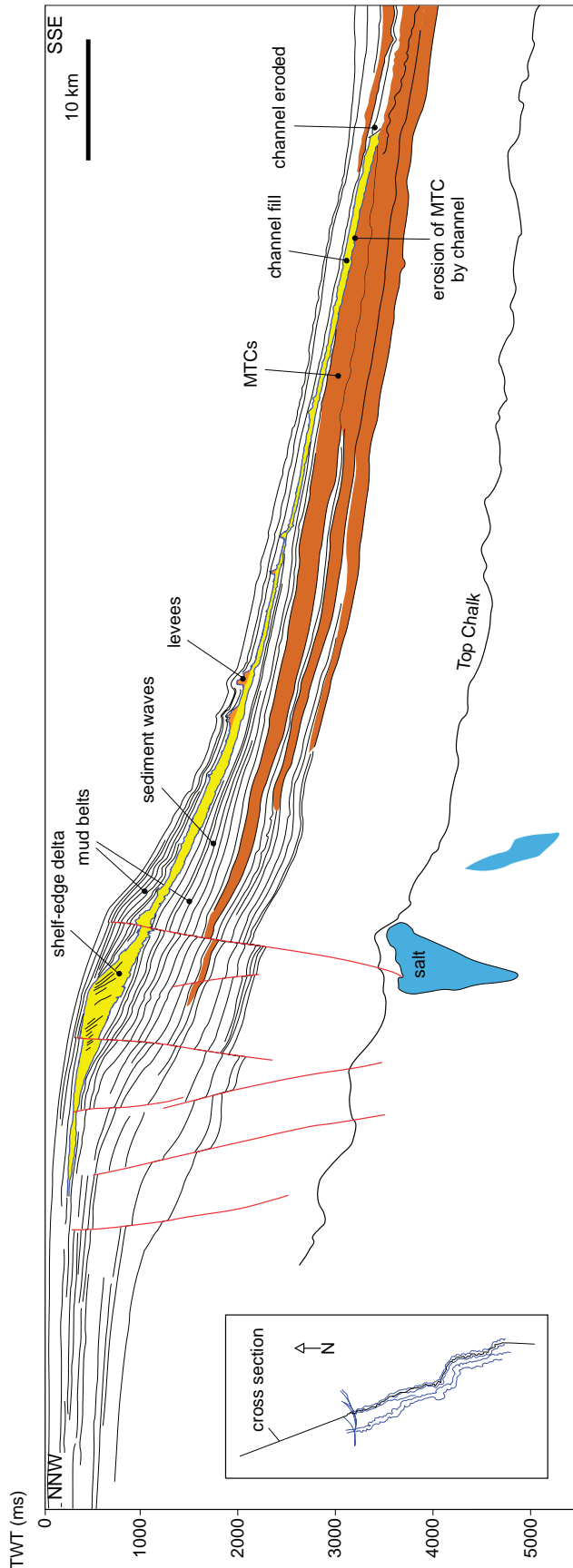FIG. 28.—Line drawing of seismic section along axis of Einstein channel, from the shelf to the present-day abyssal plain.

system suggests that partitioning of sand between the shelf-edge depocenter and deep-marine turbidites is not so dichotomic: significant amounts of sand can be deposited in the delta, on the slope, and on the basin floor at the same time. If mouth-bar sediment failure is considered an important source of sediment for channelized gravity flows, it is likely that a critical clinoform slope must be reached before this process becomes efficient. This would also mean that, for efficient transfer of sand from the river to the ocean, the shelf-edge delta must reach a critical size before the clinoform slope is large enough to generate turbidity currents capable of carrying sand over great distances. The observation that only large delta lobes are associated with submarine channels supports this interpretation. The fact that large delta lobes are required for the development of large submarine channels also implies that significant sand accumulations on the slope and at the toe of slope can occur only downdip from well-developed shelf-edge deltas.

Relationships between Slope Profile and Depositional Processes

Slope topography is the result of the interplay between erosion, sedimentation, and deformation; in turn, the spatial distribution of erosion and deposition by sediment gravity flows is strongly influenced by subtle changes in gradient. In the northeastern Gulf of Mexico, sedimentary processes seem to play the main role in determining overall slope topography.

The seismic geometries and patterns described here suggest that the most important sedimentary processes include (1) laterally extensive, dilute turbidity currents generated either through convective instabilities in the hypopycnal plumes or from wave- and current-supported near-seabed suspensions; such flows can probably generate sediment waves and incipient slope gully fields; (2) turbidity currents derived from mouth-bar failures on the fronts of shelf-edge deltas; these are likely to be relatively narrow, usually channelized and denser, more sand-rich flows that probably shape the slope channels; and (3) large translational slides and slumps that originate on the upper slope and deposit mass-transport complexes lower on the slope.

Mud belts dominate the upper slope, but mass-transport complexes are predominant farther downdip. Apart from the "real" shelf-edge delta fronts, the downdip sides of the mud belts form the steepest slopes, often exceeding 3° (Fig. 29A). These are areas prone to sediment failure (e.g., Figs. 2, 25).

A larger-scale view of continental slope-profiles typical of the northeastern Gulf of Mexico (Figs. 28, 29A) suggests that there is a reduction in slope from the upper-slope mud belts to the area dominated by mass-transport deposits. Sediment slides and slumps come to rest on steeper slopes than do the much more mobile turbidity currents. Their stacked deposits in the northeastern Gulf of Mexico form average slopes of about 1° (Fig. 29A). The change in slope associated with the updip end of the MTC-dominated section is the likely cause for the deposition of submarine aprons perched on the slope as seen along the Fuji and Einstein channels (Figs. 16, 22).

Another significant change occurs at the toe of slope (Fig. 29A), where gradients drop below ~ 0.4°. This is an area dominated by deposition from turbidity currents and other sediment gravity flows; most of the sand that passes through the slope channels like Fuji and Einstein must be deposited in this setting.

Overall, the upper and middle parts of the slope in the northeastern Gulf of Mexico are relatively steep. Once a smooth thalweg profile is reached in a channel, the majority of large turbidity currents capable of carrying significant amounts of sand are unlikely to deposit most of their sediment load before
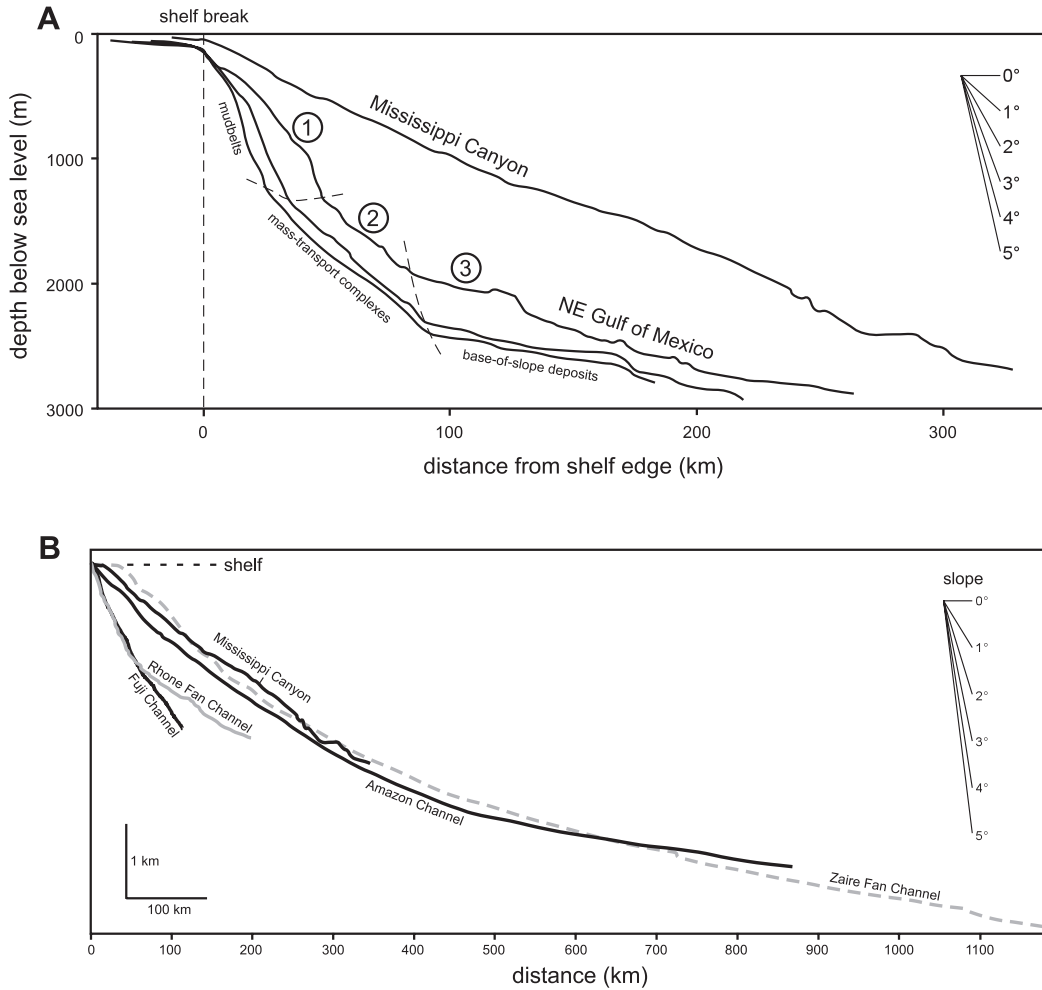
Fig. 29.— **A)** Topographic profiles characteristic of the slope in the northeastern Gulf of Mexico. Locations of profiles are shown in Figure 1. Circled numbers correspond to slope types discussed in text. **B)** Comparison of thalweg profiles for a number of submarine channels. Data are from Pirmez and Imran (2003)—Amazon Channel; Torres et al. (1997)—Rhone Fan Channel; and Babonneau et al. (2002)—Zaire Fan Channel.

reaching the toe of slope. Compared to other submarine channels (Fig. 29B), Fuji and Einstein have steep thalwegs, with gradients that are present in only the upper reaches of the canyon in large submarine fan systems like the Amazon or Zaire. The upper part of the Rhone Fan Channel has slopes similar to those of Fuji Channel (Fig. 29B), until the point where the Rhone Fan Channel reaches the toe of slope and fan deposition starts. Here the gradient drops and becomes similar to slopes in other major submarine fan channels. Thus, the mapped lengths of Fuji and Einstein channels should be viewed as largely erosional, bypass features, incipient to submarine valley formation.

This view is supported by the bulk sediment volumes deposited in the two channels (Fig. 30). These volumes were estimated using depth-converted seismic horizons at the bases and tops of the channels, levees, and delta. Although only a fraction of the sediment volume in the shelf-edge delta is present in the slope channels, the total sediment volume deposited on the slope equals that of the delta, and channel–levee deposition, in addition to mud belts, is an important process that contributes to the progradation of the upper slope in the eastern Gulf of Mexico.

CONCLUSIONS

1. The Pleistocene Fuji–Einstein system in the northeastern Gulf of Mexico consists of a shelf-edge delta with coeval gullies and submarine channel–levee systems on the slope in front of it. Seismic reflections are continuous from the prodelta clinoforms of the Fuji–Einstein delta to overbank and slope deposits adjacent to the Fuji and Einstein channels.

2. Stratal architectures and offlap-break trajectories suggest that the Fuji–Einstein delta and time-equivalent deposits on the slope developed during a single cycle of falling-to-rising sea level. Based on its burial depth, stratal position relative to other shelf-edge deltas, and the present-day depth of the offlap break during maximum regression, delta progradation is estimated to have taken place during one of the sea-level lowstands of marine isotope stages 12 to 20.

3. The Fuji–Einstein delta consists of five smaller delta lobes. The absence of an incised valley on the outermost shelf suggests that delta-lobe switching was the result of autocyclic processes.
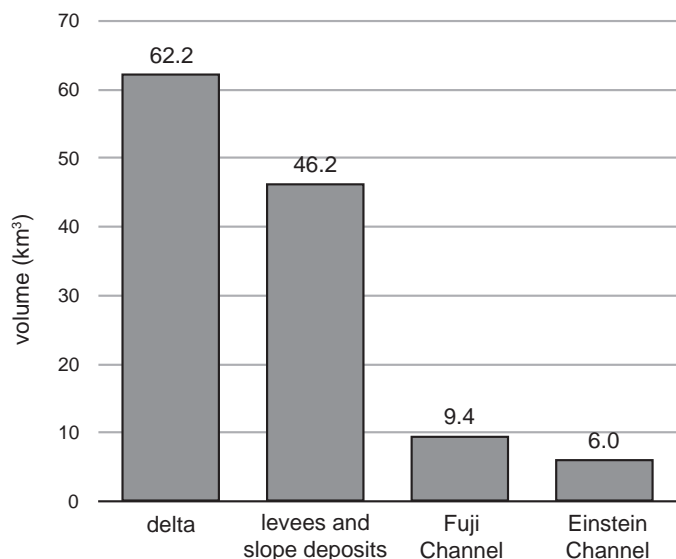
FIG. 30.—Estimated bulk sediment volumes of different parts of the Fuji–Einstein system.

4. Each fluvial avulsion and corresponding delta-lobe shift corresponds to the formation of a new gully field on the upper slope. Gully fields are present at the base and top of the Fuji–Einstein delta and at the interfaces between delta lobes. They appear to be initiated at the onset of delta lobe switching. Outboard of the two largest lobes, one of the larger gullies in the middle of the gully field captures most of the flows and evolves into a larger leveed channel. Channel growth appears to have been particularly active during the latter stages of delta-lobe progradation.

5. The Fuji and Einstein slope channels are deeply incised into the shelf-edge delta, but the absence of a single, easily mappable erosional surface separating channel-fill deposits from underlying deltaic deposits indicates that delta progradation was coeval with slope-channel development. After delta-lobe abandonment, the channels became largely inactive but were reoccupied later by flows supplied by small channel-head deltas.

6. Where they encounter areas with lower gradients, the larger delta-related slope channels source submarine aprons 2 to 4 km wide. Such lower-gradient areas include the footwalls of counter-regional growth faults, and the transition zone from upper-slope shales to areas dominated by mass-transport deposits. If the slope gully remains active for a long enough time, its corresponding submarine apron smooths out the slope and becomes incised by later bypassing flows.

7. Channel evolution is largely driven by adjustment to a smooth equilibrium profile. Channel incision is greatest where convex-up sections of the slope are eroded to eventually reach a smooth channel thalweg profile, and it is close to zero where the initial slope topography had a concave-up shape. Both Fuji and Einstein channels formed through migration of a single channel form 500 m wide, in parallel with variable amounts of incision.

High-resolution seismic images related to this study can be found at the Virtual Seismic Atlas website:

Channel-levee systems linked to shelf-edge delta, Gulf of Mexico (http://see-atlas.leeds.ac.uk:8080/homePages/generic. jsp?resourceId=0900006480015f8d)

REFERENCES

ABREU, V., SULLIVAN, M., PIRMEZ, C., AND MOHRIG, D.C., 2003, Lateral accretion packages (LAPs): an important reservoir element in deep water sinuous channels: Marine and Petroleum Geology, v. 20, p. 631–648.

ADEOGBA, A.A., MCHARGUE, T.R., AND GRAHAM, S.A., 2005, Transient fan architecture and depositional controls from near-surface 3-D seismic data, Niger Delta continental slope: American Association of Petroleum Geologists, Bulletin, v. 89, p. 627–643.

AKSU, A.E., AND PIPER, D.J.W., 1983, Progradation of the late Quaternary Gediz delta, Turkey: Marine Geology, v. 54, p. 1–25.

ANDERSON, J.B., AND FILLON, R., 2004, Late Quaternary Stratigraphic Evolution of the Northern Gulf of Mexico Margin: SEPM, Special Publication 79, 311 p.

BABONNEAU, N., SAVOYE, B., CREMER, M., AND KLEIN, B., 2002, Morphology and architecture of the present canyon and channel system of the Zaire deep-sea fan: Marine and Petroleum Geology, v. 19, p. 445–467.

BERRYHILL, H.L., SUTER, J.R., AND HARDIN, N.S., 1986, Late Quaternary Facies and Structure, Northern Gulf of Mexico: American Association of Petroleum Geologists, Studies in Geology, v. 23, 289 p.

BURGESS, P.M., AND HOVIUS, N., 1998, Rates of delta progradation during highstands: consequences for timing of deposition in deep-marine systems: Geological Society of London, Journal, v. 155, p. 217–222.

CATTANEO, A., CORREGGIARI, A., LANGONE, L., AND TRINCARDI, F., 2003, The late-Holocene Gargano subaqueous delta, Adriatic shelf: Sediment pathways and supply fluctuations: Marine Geology, v. 193, p. 61–91.

CATTANEO, A., CORREGGIARI, A., MARSSET, T., THOMAS, Y., MARSSET, B., AND TRINCARDI, F., 2004, Seafloor undulation pattern on the Adriatic shelf and comparison to deep-water sediment waves: Marine Geology, v. 213, p. 121–148.

CATUNEANU, O., 2006, Principles of Sequence Stratigraphy: Amsterdam, Elsevier, 376 p.

CLEMENCEAU, G.R., 1995, Ram/Powell Field; Viosca Knoll Block 912, deepwater Gulf of Mexico, in Winn, R.D., Jr., and Armentrout, J.M., eds., Turbidites and Associated Deep-Water Facies: SEPM ,Core Workshop 20, p. 95–129.

CORREGGIARI, A., TRINCARDI, F., LANGONE, L., AND ROVERI, M., 2001, Styles of failure in Late Holocene highstand prodelta wedges on the Adriatic shelf: Journal of Sedimentary Research, v. 71, p. 218–236.

CUMMINGS, D.I., ARNOTT, R.W.C., AND HART, B.S., 2003, Seismic and sequence stratigraphy of a braided fluvial sheet, Lower Cretaceous Missisauga Formation, offshore Nova Scotia, Canada: Implications for deep-water exploration, in Roberts, H.H., Rosen, N.C, Fillon, R.H., and Anderson, J.B., eds., Shelf Margin Deltas and Linked Down Slope Petroleum Systems: Global Significance and Future Exploration Potential: Gulf Coast Section SEPM Foundation, 23rd Annual Bob F. Perkins Research Conference, p. 647–665.

DEPTUCK, M.E., STEFFENS, G.S., BARTON, M., AND PIRMEZ, C., 2003, Architecture and evolution of upper fan channel-belts on the Niger Delta slope and in the Arabian Sea: Marine and Petroleum Geology, v. 20, p. 649–676.

DEPTUCK, M.E., SYLVESTER, Z., PIRMEZ, C., AND O'BYRNE, C., 2007, Migration–aggradation history and 3-D seismic geomorphology of submarine channels in the Pleistocene Benin-Major Canyon, western Niger delta slope: Marine and Petroleum Geology v. 24, p. 406–433.

DEPTUCK, M.E., PIPER, D.J.W., SAVOYE, B., AND GERVAIS, A., 2008, Dimensions and architecture of Late Pleistocene submarine lobes off the northern margin of east Corsica: Sedimentology, v. 55, p. 869–898.

FARRE, J.A., MCGREGOR, B.A., RYAN, W.B.F., AND ROBB, J.M., 1983, Breaching the shelfbreak: Passage from youthful to mature phase in submarine

canyon evolution, *in* Stanley, D.J., and Moore, G.T., eds., The Shelfbreak; Critical Interface on Continental Margins: SEPM, Special Publication 33, p. 25–39.

FAULKENBERRY, L., 2004, High-resolution seismic architecture of upper slope submarine channel and canyon systems: Gulf of Mexico and offshore Nigeria: Ph.D. Thesis, University of Leeds, 270 p.

FILLON, R.H., KOHL, B., AND ROBERTS, H.H., 2004, Late Quaternary deposition and paleobathymetry at the shelf–slope transition, ancestral Mobile River delta complex, northeastern Gulf of Mexico, *in* Anderson, J.B., and Fillon, R.H., eds., Late Quaternary Stratigraphic Evolution of the Northern Gulf of Mexico Margin: SEPM, Special Publication 79, p. 111-141.

FRATICELLI, C.B., AND ANDERSON, J.B., 2003, The impact of the Brazos deltaic system on upper slope stratigraphic sequence evolution, *in* Roberts, H.H., Rosen, N.C., Fillon, R.H., and Anderson, J.B., eds., Shelf Margin Deltas and Linked Down Slope Petroleum Systems: Global Significance and Future Exploration Potential: Gulf Coast Section SEPM Foundation, 23rd Annual Bob F. Perkins Research Conference, p. 325–357.

GARDNER, J.V., CALDER, B.R., HUGHES CLARKE, J.E., MAYER, L.A., ELSTON, G., AND RZHANOV, Y., 2007, Drowned shelf-edge deltas, barrier islands and related features along the outer continental shelf north of the head of De Soto Canyon, NE Gulf of Mexico: Geomorphology v. 89, p. 370–390.

GEE, M.J.R., AND GAWTHORPE, R., 2007, Early evolution of submarine channels offshore Angola revealed by three-dimensional seismic data, *in* Davies, R.J., Posamentier, H.W., Wood, L.J., and Cartwright, J.A., eds., Seismic Geomorphology: Applications to Hydrocarbon Exploration and Production: Geological Society of London, Special Publication 277, p. 223–235.

GERVAIS, A., SAVOYE, B., AND PIPER, D.J.W., 2004, Present morphology and depositional architecture of a sandy confined submarine system: the Golo turbidite system (eastern margin of Corsica), *in* Lomas, S.A., and Joseph, P., ed., Confined Turbidite Systems: Geological Society of London, Special Publication 222, p. 59–59.

GODO, T.J., 2006, Identification of stratigraphic traps with subtle seismic amplitude effects in Miocene channel/levee sand systems, NE Gulf of Mexico, *in* Allen, M.R., Goffey, G.P., Morgan, R.K., and Walker, I.M., eds., The Deliberate Search for the Stratigraphic Trap: Geological Society of London, Special Publication 254, p. 127–151.

HACKBARTH, C.J., AND SHEW, R.D., 1993, Interpretation of a mid-Pleistocene leveed channel system using high-resolution seismic data, cores, and logs, Viosca Knoll, northeastern Gulf of Mexico (abstract): American Association of Petroleum Geologists, Annual Meeting Abstracts, p. 112.

HACKBARTH, C.J., AND SHEW, R., 1994, Morphology and stratigraphy of a mid-Pleistocene turbidite leveed channel from seismic, core and log data, Northeastern Gulf of Mexico: Gulf Coast Section SEPM Foundation, 15th Annual Research Conference, Submarine Fans and Turbidite Systems, p. 127–135.

HART, B.S., PRIOR, D.B., BARRIE, J.V., CURRIE, R.G., AND LUTERNAUER, J.L., 1992, A river mouth submarine channel and failure complex, Fraser Delta, Canada: Sedimentary Geology, v. 81, p. 73–87.

HILL, P.R., CONWAY, K., LINTERN, D.G., MEULÉ, S., PICARD, K., AND BARRIE, J.V., 2008, Sedimentary processes and sediment dispersal in the southern Strait of Georgia, B.C., Canada: Marine Environmental Research, v. 66, p. S39–S48.

HILL, P.S., FOX, J.M., CROCKETT, J.S., CURRAN, K.J., FRIEDRICHS, C.T., GEYER, W.R., MILLIGAN, T.G., OGSTON, A.S., PUIG, P., AND SCULLY, M.E., 2007, Sediment delivery to the seabed on continental margins, *in* Nittrouer, C.A., Austin, J.A., Field, M.E., Kravitz, J.H., Syvitski, J.P.M., and Wiberg, P.L., eds., Continental Margin Sedimentation: From Sediment Transport to Sequence Stratigraphy: International Association of Sedimentologists, Special Publication 37, p. 49–99.

KENDRICK, J. W., 2000, Turbidite reservoir architecture in the northern Gulf of Mexico deepwater: Insights from the development of Auger,

Tahoe, and Ram/Powell fields, *in* Weimer, P., Slatt, R.M., Coleman, J.H., Rosen, N.C., Nelson, H., Bouma, A.H., Styzen, M.J., and Lawrence, D.T., eds., Deep-Water Reservoirs of the World: Gulf Coast Section SEPM Foundation, 20th Annual Bob F. Perkins Research Conference, p. 450–468.

KUEHL, S.A., LEVY, B.M., MOORE, W.S., AND ALLISON, M.A., 1997, Subaqueous delta of the Ganges–Brahmaputra river system: Marine Geology, v. 144, p. 81–96.

LISIECKI, L.E., AND RAYMO, M.E., 2005, A Pliocene–Pleistocene stack of 57 globally distributed benthic ^{18}O records: Paleoceanography v. 20, p, 1–17.

McBRIDE, R.A., MOSLOW, T.F., ROBERTS, H.H., AND DIECCHIO, R.J., 2004, Late Quaternary geology of the northeastern Gulf of Mexico shelf: sedimentology, depositional history, and ancient analogs of a major shelf sand sheet of the modern transgressive systems tract, *in* Anderson, J.B., and Fillon, R.H., eds., Late Quaternary Stratigraphic Evolution of the Northern Gulf of Mexico Margin: SEPM, Special Publication 79, p. 55–83.

MECKEL, L.D., 2003, Shelf margin deltas: the key to big reserves, *in* Roberts, H.H., Rosen, N.C., Fillon, R.H., and Anderson, J.B., eds., Shelf Margin Deltas and Linked Down Slope Petroleum Systems: Global Significance and Future Exploration Potential: Gulf Coast Section SEPM Foundation, 23rd Annual Bob F. Perkins Research Conference, p. 167–204.

MELLERE, D., PLINK-BJÖRKLUND, P., AND STEEL, R., 2002, Anatomy of shelf deltas at the edge of a prograding Eocene shelf margin, Spitsbergen: Sedimentology, v. 49, p. 1181–1206.

MITCHELL, N.C., 2005, Channelled erosion through a marine dump site of dredge spoils at the mouth of the Puyallup River, Washington State, U.S.A.: Marine Geology, v. 220, p. 131–151.

MULDER, T., AND SYVITSKI, J.P.M., 1995, Turbidity currents generated at river mouths during exceptional discharges to the world oceans: Journal of Geology, v. 103, p. 285–299.

MYERS, K.J., AND MILTON, N.J., 1996, Concepts and principles of sequence stratigraphy, *in* Emery, D., and Myers, K.J., eds., Sequence Stratigraphy: Oxford, U.K., Blackwell Scientific Publications, p. 11–41.

NITTROUER, C.A., KUEHL, S.A., DEMASTER, D.J., AND KOWSMANN, R.O., 1986, The deltaic nature of Amazon shelf sedimentation: Geological Society of America, Bulletin, v. 97, p. 444–458.

NORMARK, W.R., HESS, G.R., STOW, D.A.V., AND BOWEN, A.J., 1980, Sediment waves on the Monterey Fan levee: a preliminary physical interpretation: Marine Geology, v. 37, p. 1–18.

NORMARK, W.R., PIPER, D.J.W., POSAMENTIER, H., PIRMEZ, C., AND MIGEON, S., 2002, Variability in form and growth of sediment waves on turbidite channel levees: Marine Geology, v. 192, p. 23–58.

PARSONS, J.D., BUSH, J.W.M., AND SYVITSKI, J.P.M., 2001, Hyperpycnal plume formation from riverine outflows with small sediment concentrations: Sedimentology, v. 48, p. 465–478.

PETTINGILL, H.S., AND WEIMER, P., 2002, Worldwide deepwater exploration and production: Past, present, and future: The Leading Edge, v. 21, p. 371-376.

PIRMEZ, C., AND FLOOD, R.D., 1995, Morphology and structure of Amazon channel, *in* Flood, R.D., Piper, D.J.W., and Klaus, A., eds., Proceedings of the Ocean Drilling Program, Initial Reports, v. 155, p. 23–45.

PIRMEZ, C., AND IMRAN, J., 2003, Reconstruction of turbidity currents in the Amazon Channel: Marine and Petroleum Geology, v. 20, p. 823–849.

PIRMEZ, C., BEAUBOUEF, R.T., FRIEDMANN, S.J., AND MOHRIG, D.C., 2000, Equilibrium profile and baselevel in submarine channels: examples from Late Pleistocene systems and implications for architecture in deepwater reservoirs, *in* Weimer, P., Slatt, R.M., Coleman, J.H., Rosen, N.C., Nelson, H., Bouma, A.H., Styzen, M.J., and Lawrence, D.T., eds., Deep-Water Reservoirs of the World: Gulf Coast Section SEPM Foundation, 20th Annual Bob F. Perkins Research Conference, p. 782–805.

PLINK-BJÖRKLUND, P., AND STEEL, R., 2005, Deltas on falling-stage and lowstand shelf margins, the Eocene Central Basin of Spitsbergen:

Importance of sediment supply, *in* Giosan, L., and Bhattacharya, J.P., eds., River Deltas—Concepts, Models, and Examples: SEPM, Special Publication 83, p. 179–206.

Porebski, S., and Steel, R.J., 2003, Shelf-margin deltas: their stratigraphic significance and relation to deepwater sands: Earth-Science Reviews, v. 62, p. 283–326.

Posamentier, H.W., 2003, A linked shelf-edge delta and slope-channel turbidite system: 3D seismic case study from the eastern Gulf of Mexico, *in* Roberts, H.H., Rosen, N.C., Fillon, R.H., and Anderson, J.B., eds., Shelf Margin Deltas and Linked Down Slope Petroleum Systems: Global Significance and Future Exploration Potential: Gulf Coast Section SEPM Foundation, 23rd Annual Bob F. Perkins Research Conference, p. 115–134.

Posamentier, H.W., and Allen, G.P., 1993, Variability of the sequence stratigraphic model: effects of local basin factors: Sedimentary Geology, v. 86, p. 91–109.

Posamentier, H.W., Jervey, M.T., and Vail, P.R., 1988, Eustatic controls on clastic deposition I—conceptual framework, *in* Wilgus, C.K., Hastings, B.S., Kendall, C.G.St.C., Posamentier, H.W., Ross, C.A., and Van Wagoner, J.C., eds., Sea-Level Changes: An Integrated Approach: SEPM, Special Publication 42, p. 109–124.

Posamentier, H.W., Allen, G. P., James, D.P., and Tesson, M., 1992, Forced regressions in a sequence stratigraphic framework: concepts, examples, and exploration significance: American Association of Petroleum Geologists, Bulletin, v. 76, p. 1687–1709.

Prather, B.E., 2003, Controls on reservoir distribution, architecture and stratigraphic trapping in slope settings: Marine and Petroleum Geology, v. 20, p. 529–545.

Prather, B.E., Booth, J.R., Steffens, G.S., and Craig, P.A., 1998, Classification, lithologic calibration and stratigraphic succession of seismic facies from intraslope basins, deep water Gulf of Mexico, U.S.A.: American Association of Petroleum Geologists, Bulletin, v. 82, p. 701–728.

Pratson, L.F., and Coakley, B.J., 1996, A model for the headward erosion of submarine canyons induced by downslope-eroding sediment flows: Geological Society of America, Bulletin, v. 108, p, 225–234.

Rabineau, M., Berné, S., Aslanian, D., Olivet, J.L., Joseph, P., Guillocheau, F., Bourillet, J.F., Ledrezen, E., and Granjeon, D., 2005 Sedimentary sequences in the Gulf of Lion: A record of 100,000 years climatic cycles: Marine and Petroleum Geology v. 22, p. 775–804.

Roberts, H.H., Fillon, R.H., Kohl, B., Robalin, J.M., and Sydow, J.C., 2004, Depositional architecture of the Lagniappe Delta: sediment characteristics, timing of depositional events, and temporal relationship with adjacent shelf-edge deltas, *in* Anderson, J.B., and Fillon, R.H., eds., Late Quaternary Stratigraphic Evolution of the Northern Gulf of Mexico Margin: SEPM, Special Publication 79, p. 143–188.

Saller, A.H., Noah, J.T., Ruzuar, A.P., and Schneider, R., 2004, Linked lowstand delta to basin-floor fan deposition, offshore Indonesia: An analog for deep-water reservoir systems: American Association of Petroleum Geologists, Bulletin v. 88, p, 21–46.

Schwenk, T., Spieß, V., Breitzke, M., and Hübscher, C., 2005, The architecture and evolution of the Middle Bengal Fan in vicinity of the active channel–levee system imaged by high-resolution seismic data: Marine and Petroleum Geology, v. 22, p. 637–656.

Suter, J.R., and Berryhill, H.L., 1985, Late Quaternary shelf-margin deltas, northwest Gulf of Mexico: American Association of Petroleum Geologists, Bulletin v. 69, p, 77–91.

Sydow, J.C., Finneran, J., and Bowman, A.P., 2003, Stacked shelf-edge delta reservoirs of the Columbus Basin, Trinidad, West Indies, *in* Roberts, H.H., Rosen, N.C., Fillon, R.H., and Anderson, J.B., eds., Shelf Margin Deltas and Linked Down Slope Petroleum Systems: Global Significance and Future Exploration Potential: Gulf Coast Section SEPM Foundation, 23rd Annual Bob F. Perkins Research Conference, p. 441–465.

Sylvester, Z., Pirmez, C., and Cantelli, A., 2011, A model of submarine channel-levee evolution based on channel trajectories: Implications for stratigraphic architecture: Marine and Petroleum Geology, v. 28, p. 716-727. doi:10.1016/j.marpetgeo.2010.05.012.

Torres, J., Droz, L., Savoye, B., Terentieva, E., Cochonat, P., Kenyon, N.H., and Canals, M., 1997, Deep-sea avulsion and morphosedimentary evolution of the Rhone Fan Valley and Neofan during the late quaternary (north-western Mediterranean Sea): Sedimentology, v. 44, p. 457–477.

Trincardi, F., and Normark, W.R., 1988, Sediment waves on the Tiber prodelta slope: Interaction of deltaic sedimentation and currents along the shelf: Geo-Marine Letters, v. 8, 149–157.

Vakarelov, B.K., 2006, Controls on stratigraphic architecture in shallow marine environments: Tectonic forcing and mud geometries: Ph.D. Thesis, The University of Texas at Dallas, 142 p.

Vakarelov, B.K., and Bhattacharya, J.P., 2004, The missing mud belts in the ancient record (abstract): Geological Society of America, Abstracts with Programs, v. 36, no. 5, p. 461.

Winker, C.D., 1993a, Leveed slope channels and shelf-margin deltas of the Late Pliocene to middle Pleistocene Mobile river, NE Gulf of Mexico: comparison with sequence-stratigraphic models (abstract): American Association of Petroleum Geologists, 1993 Annual Convention, p. 201.

Winker, C.D., 1993b, Pleistocene lowstand deposits of the Mississippi, Mobile, and Trinity rivers: models for turbidite sedimentation in the Gulf of Mexico (abstract): American Association of Petroleum Geologists, Annual Convention Program, p. 202.

Winker, C.D., and Shipp, R.C., 2003, Sequence boundary ambiguities in shelf-margin deltas and the shelf–slope transition: Illustrations from the Pleistocene of the Gulf of Mexico, *in* Roberts, H.H., Rosen, N.C., Fillon, R.H., and Anderson, J.B., eds., Shelf Margin Deltas and Linked Down Slope Petroleum Systems: Global Significance and Future Exploration Potential: Gulf Coast Section SEPM Foundation, 23rd Annual Bob F. Perkins Research Conference, p. 309–311.